

# What goes around comes around: the US climate-economic cycle

Konstantin Boss, Alessandra Testa<sup>1</sup>

## Abstract

We use a spatial data set of US temperatures in a factor-augmented VAR to quantify the contribution of the US economy to fluctuations in temperatures over the past 70 years. We find that economic expansions do not only lead to warming: technology improvements decrease temperatures temporarily at industry-dominated locations, whereas investment and labor supply shocks increase them in the entire country and persistently. This can happen when the cooling effect of aerosol emissions initially outweighs the warming effect from greenhouse gases, as is the case for technology shocks, but not for investment and labor supply shocks. Taken together, these economic shocks explain around 25% of long-term temperature variation in the US. In turn, neither the human-induced nor the naturally occurring temperature changes have had any significant effect on aggregate US GDP.

**Keywords:** Factor-Augmented VAR, Climate Econometrics, Temperature Shocks, Frequency Domain Identification

*JEL classification:* C32, C38, Q54

---

<sup>1</sup>Boss: Universitat Autònoma de Barcelona (UAB) and Barcelona School of Economics, konstantin.boss@bse.eu; Testa: Università di Bologna, Collegio Carlo Alberto, and UAB, alessandra.testa@carloalberto.org. Boss acknowledges funding under the FPI grant PRE2020-093941 of the Ministerio de Trabajo y Economía Social in Spain. We would like to thank Luca Gambetti, Sarah Zoi, Marco Mazzali, Selim Elbadri and seminar participants at the 64th Annual Conference of the Italian Economic Association (Società Italiana di Economia -SIE), the Banco de España, the Ruhr Graduate School Doctoral Conference, Dynamic Econometrics at Oxford, the JRC, as well as of the Bellaterra Macro Club for their very valuable comments.

# 1 Introduction

The rise in global socio-economic activity and the accompanying increase in anthropological greenhouse gas (GHG) emissions that characterized the past century are thought to be the dominant causes of global warming. Worldwide average surface temperatures have already increased by  $1.1^{\circ}\text{C}$  since the industrial revolution and are projected to increase by between  $1.4^{\circ}\text{C}$  and  $4.4^{\circ}\text{C}$  until 2100 (IPCC, 2023). In turn, temperature increases can lead to lower agricultural yields (Deschênes & Greenstone, 2007), more premature deaths (Barreca et al., 2015), and diminished productivity (Burke et al., 2015), resulting in potentially severe losses in welfare.

In this chapter we develop an empirical framework for the United States (US) to study how economic activity has affected temperatures and vice versa. We use a factor-augmented vector autoregression (FAVAR, Bernanke et al. (2005)) to model the dynamics of US temperatures on a  $0.5^{\circ} \times 0.5^{\circ}$  spatial grid together with key macroeconomic aggregates. To disentangle the effect of human activity on temperatures from the effect of temperatures on human activity, we rely on the notion of structural shocks that is common in causal macroeconomic inference (Ramey, 2016). We use partial identification techniques to pin down three well-established economic shocks in the frequency domain along the lines of Forni et al. (2023). First, a technology shock is identified as the main contributor to low frequency variation in utilization-adjusted TFP, similar to DiCecio & Owyang (2010) and Dieppe et al. (2021). Second, conditional on the technology shock, we identify an investment shock in the spirit of Justiniano et al. (2010) and Auclert et al. (2020) as the main driver of business-cycle fluctuations in investment. Third, similar to Shapiro & Watson (1988) we identify a labor supply shock as the main driver of the low frequency component of hours worked, conditional on both the technology and the investment shock. On the other hand, we rely on statistical arguments to identify temperature shocks. As Angeletos et al. (2020) identify an economic “main business-cycle shock”, we apply a similar reasoning to capture the main drivers of temperature fluctuations in specific geographic areas, such as the west coast, the east coast, the Gulf region or the non-coastal states, as well as in specific frequency bands, for example at the El Niño-La Niña periodicities. We then compute the impulse responses of US real GDP to these shocks.

Based on our analysis, we report the following qualitative results: first, it is insufficient to rely on a single measure of national temperatures such as (weighted) averages, as is frequently done in the literature (Dell et al., 2012), (Burke et al., 2015), (Acevedo et al., 2020). This is because there is a lower bound of five large shocks driving US temperatures. Average temperatures alone only reflect variation in the Midwest region and neglect temperature changes in the economically important coastal areas. This happens because the American Midwest is affected by strong cold air flows from the North and warm air flows from the South leading to very high temperature variability (Kunkel et al., 2013). Geographic heterogeneity also matters for the effect of temperatures on aggregate GDP, a crucial relationship for environmental policy-making: if warming affects only the west of the country, this can be net positive for the economy, whereas temperature increases generally diminish output slightly. Second, we provide evidence for a relationship between temperatures and socio-economic activity mostly through changes in TFP.

A loss in productivity is thought to be one of the main channels for the negative effects of temperature warming (Burke et al., 2015). We argue along the lines of Pretis (2021) that it is important to properly distinguish if temperature fluctuations cause productivity changes or vice versa. In the case of the US, we find that the negative co-movement between temperatures and TFP is caused by economic shocks.

In addition, we contribute the following quantitative findings to the literature: first, on average, a quarter of the low frequency component of US temperatures can be attributed to the three economic shocks with technology shocks accounting for 10%, investment shocks for 11%, and labor supply shocks for 4%. In the east and south of the US, where manufacturing and natural resource processing are concentrated, the explained variation from technology shocks alone can be as high as 35%. High and medium cycle variations of temperatures, on the other hand, are not strongly explained by the economic shocks. The economic shocks have small, yet persistent effects on temperatures. While technology shocks decrease temperatures, investment shocks and labor supply shocks lead to geographically homogeneous warming, in the area of  $0.01^{\circ}\text{C}$ . We argue that decreases in temperatures can be explained by a stronger effect of aerosol emissions than GHG emissions, whereas heating is observed when aerosols are removed and GHGs emitted. Second, central US and east coast centered increases of  $1^{\circ}\text{C}$  lead to mild losses of aggregate GDP around  $0.1\% - 0.13\%$ , echoing the findings in Natoli (2023). However, shocks that predominantly affect temperatures on the west coast can have expansionary effects. We find them to lead to up to 0.29% higher GDP after an initial decrease of around 0.32%. This is because when increases in temperatures occur in the west, they are accompanied by decreases in the east. The net effect of this is positive for aggregate real GDP. Temperature shocks are not persistent for temperatures anywhere in the US. Third, we carry out a counterfactual exercise to assess how anthropologically induced temperature changes spill back into the economy. We show that GDP would only be fractionally higher, if this mechanism is essentially nullified. This implies that the US economy – at least in our sample – has not been heavily influenced by human-made temperature changes. This is in line with the view that the US for the most part has been close to a bliss-point where temperature warming has so far had essentially zero aggregate effects (see e.g. Dell et al. (2012) or Nath et al. (2023)).

Comprehensive overviews of the climate-econometric literature are provided by Newell et al. (2021) and de Juan et al. (2022). We relate to and expand the literature that quantifies the effect of temperatures on the US economy. Important contributions over the existing empirical literature are as follows: we identify the direct effect on temperatures of economic shocks that explain the bulk of macroeconomic fluctuations. This is necessary because policy oriented models such as Cai & Lontzek (2019) focus on damages from temperature changes induced by such economic shocks on the economy, although usually focusing on TFP shocks alone. In addition, we allow the data to determine the timing of the effects of emissions on temperatures rather than assuming that economic activity translates into temperature changes with a delay of a year, as is customary in the literature (e.g. Donadelli et al. (2017) or Goulet Coulombe & Göbel (2021), since this is not supported by climate research (e.g. Joos et al. (2013) or Forster et al. (2020)). Instead, we propose an identification based on statistical arguments with no implied timing restrictions.

Other studies in this area use mostly panel regressions without dynamic causal response estimates (e.g. Deryugina & Hsiang (2014), Colacito et al. (2019), Gourio & Fries (2020)), which are uninformative about the transmission mechanism of temperature fluctuations to the real economy. Kaufmann et al. (2013), Montamat & Stock (2020), and Stock (2020) discuss economic processes affecting climate forcing (and thus temperatures), but do not identify the stochastic processes explicitly. Empirical studies that compute the effects of economic shocks on US CO<sub>2</sub> emissions are Khan et al. (2019), Fosten (2019) and Bennedsen et al. (2021), however, no explicit connection temperature changes is made. Since the effect of economic activity on temperatures is not exclusively driven by GHG emissions, but also other gases such as aerosols, Magnus et al. (2011), Storelvmo et al. (2016), Phillips et al. (2020) provide a breakdown of the respective warming and cooling effects. We show that the aerosol cooling effect prevails for technology shocks, whereas other business cycle shocks lead to warming through a dominant impulse of GHGs. From a methodological view our paper is closely related to Mumtaz & Marotta (2023), Berg et al. (2023) and Bastien-Olvera et al. (2022). The first two for the authors' use of a factor structure for temperature dynamics and the third one for the frequency domain decomposition of temperatures. While Mumtaz & Marotta (2023) use global data to characterize patterns of aggregate temperature movements, their study focuses on correlations with economic development indicators. We provide causal interpretations for the variations in temperature data and vice versa. Berg et al. (2023) consider only a single factor for their global data set, whereas we show that this captures a very localized temperature phenomenon. Bastien-Olvera et al. (2022) regress GDP growth onto the low-frequency component of average temperatures extracted using a low-pass filter. However, as we show, this component is substantially affected by economic shocks, for which the authors do not control.

The rest of the paper is organised as follows: section 2 describes the temperature and economic data we use in the empirical model, section 3 introduces the model and explains the identification methodology, section 4 presents the findings, which are discussed in section 5, together with a counterfactual exercise to assess the cost of anthropological warming and section 6 concludes.

## 2 Data

Temperature data are obtained from the *Terrestrial Air Temperature and Precipitation 1900 – 2017 Gridded Monthly* data set (Matsuura & Willmott, 2018) which provides monthly mean temperatures over land at  $0.5 \times 0.5$  degree resolution for the entire globe. The authors compute the monthly average gridded data from daily weather station records, considering only stations for which no more than five daily data points in a given month are missing. The grid cell data are estimated from measurement station averages through spatial interpolation. Outliers and unrealistic values that might arise due to measurement error are removed by the authors.

3,325 of the grid points are located in the contiguous United States (i.e. excluding Alaska, Hawaii and the US territories). We aggregate the monthly data to quarterly frequency by taking the average over the three months in a quarter and seasonally adjust

each time series using the `deseason()` function of the MATLAB Climate Data Toolbox (Greene et al., 2019), which centers and linearly detrends each time series and then removes the climatology, i.e. the average of each given month in a year. In addition, we weight each grid point by the square root of the cosine of the latitude in the center of the cell. This is common practice in the literature that computes empirical orthogonal functions (EOFs) from climate data (Hannachi et al., 2007) and serves as a means to account for the arc of the earth which changes the size of degree-based grid cells further away from the equator relative to those that are closer to the equator. EOFs are in essence the loadings of the principal components computed for gridded climate data which can be used to detect patterns such as the El Niño Southern Oscillation (ENSO) (Erichson et al., 2020).

We use this method to summarize the information contained in the gridded land surface temperature data set. To determine the number of principal components we use the criterion of Alessi et al. (2010), which suggests between 8 and 17. For parsimony, we set the number of principal components to  $r = 8$  and study the effect of picking  $r = 17$  in a robustness exercise. Figure 1 shows that the time series for average US temperature and the first principal component from our data set are 96% correlated. In addition, Figure 2 shows that the first principal component – which carries the same signal as the average – explains temperature variation only in the Midwest of the US, important economic centres such as the coastal areas are much less well explained. Similar results appear in other large countries of the world, but are not reported here. Therefore, the information in average temperatures is covered by a single principal component, which is clearly insufficient to capture the full temperature dynamics of the US. Any approach using nationwide averages will miss important spatial temperature information.

**Figure 1:** Average temperatures in the US and first principal component. Correlation is 96%.

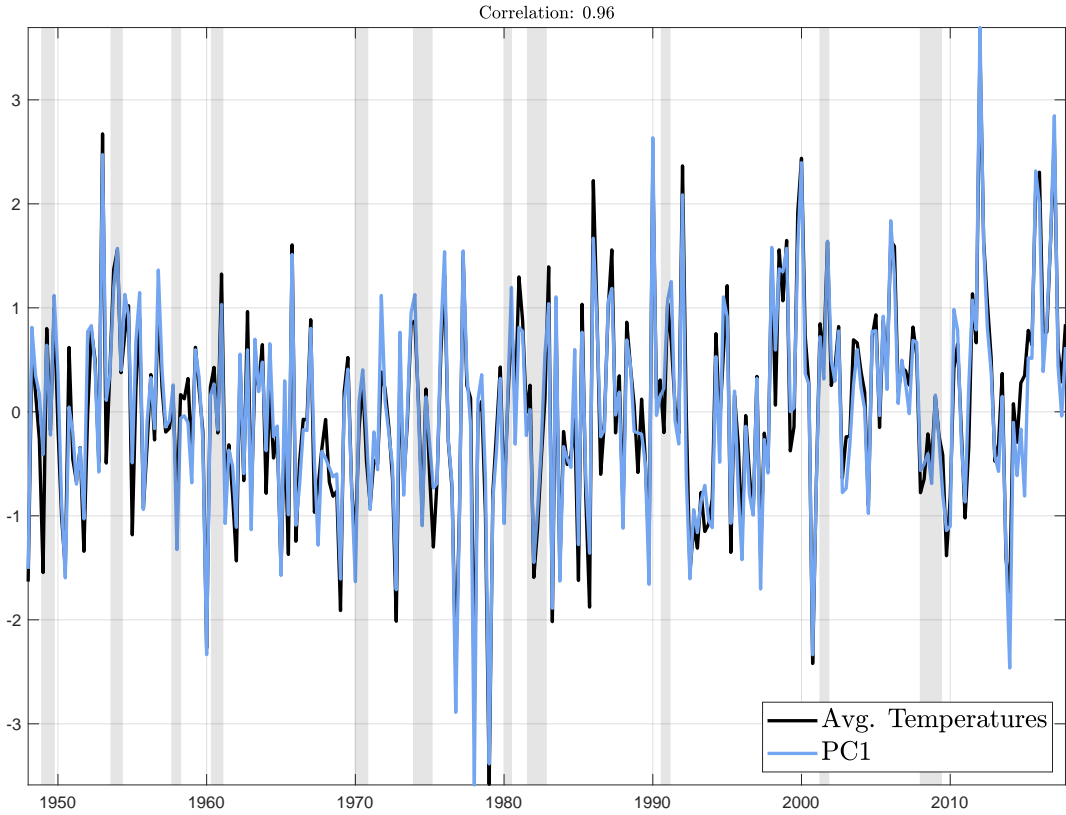
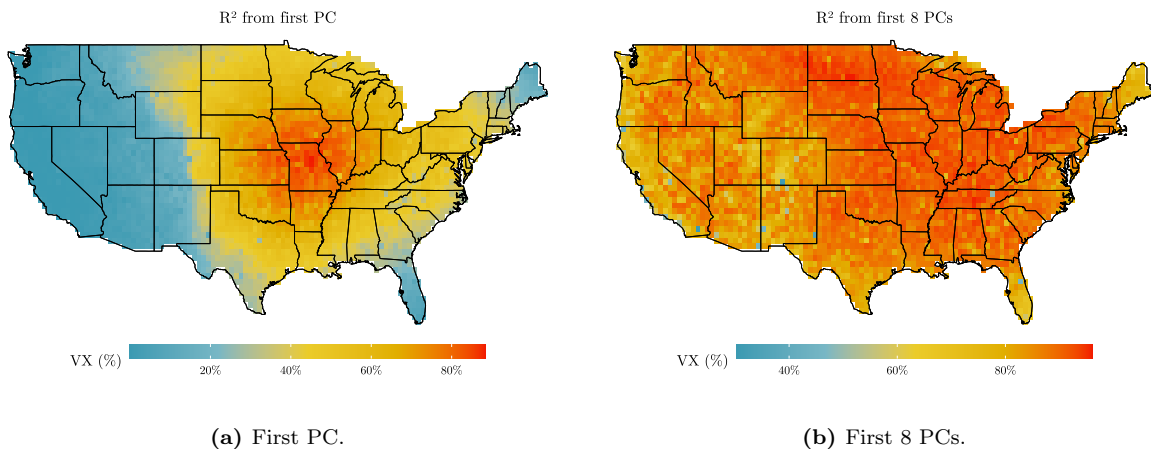


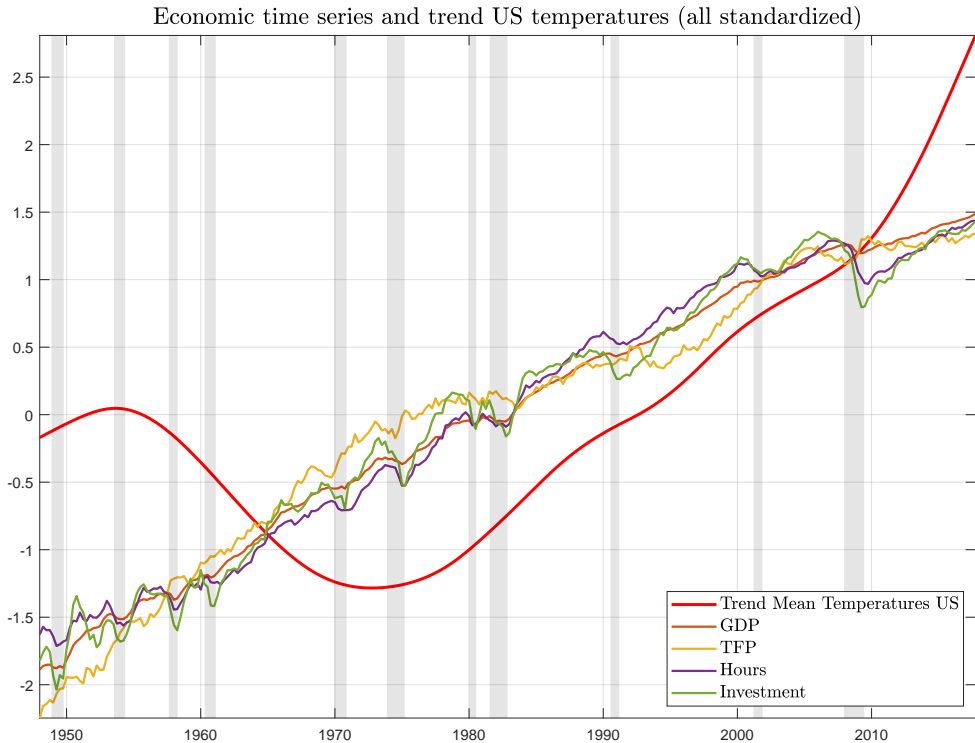
**Figure 2:**  $R^2$  from regression of grid cell temperatures on principal components.



The economic data we include are real GDP, real investment, nonfarm-business sector hours worked obtained from FRED and utilization-adjusted TFP (from Fernald (2014)). All economic variables enter the model in log-levels to account for the possibility of co-integration among economic and climate variables pointed out in Pretis (2020). We have checked the model in per-capita terms and found no major difference. A detailed account of all the economic data used in this chapter and their construction is given in the Appendix. The sample we use for estimation of the baseline model runs at quarterly

frequency from 1948:Q1 to 2017:Q4. Figure 3 plots the economic data together with the trend in average US temperatures. Temperatures exhibit an initial decrease until around the 1970s after which they trend upwards. The series appear to share a common trend as of the 1970s, but diverge again after the Great Recession where the growth rate in temperatures speeds up.

**Figure 3:** HP-filtered trend in mean contiguous US temperatures ( $\lambda = 160000$ ) and logarithmized economic time series. Shaded areas are NBER recessions. All data are centered and scaled to have zero mean and unit variance.



### 3 Econometric methodology

#### 3.1 Reduced form data representation

Our estimation procedure is carried out in two steps, as in factor-augmented vector autoregressions (FAVAR) (e.g. Bernanke et al. (2005)) and dynamic factor models (DFM) (e.g. Forni et al. (2009)). These models have the advantage that they can accommodate data sets with many time series and allow for the straightforward identification of structural shocks and their propagation through the methods common in the literature on structural VARs (SVARs) (Ramey, 2016).

The model for the temperatures at grid cell  $i$  at time  $t$  is given by

$$T_{it} = \lambda_i Y_t + \eta_{it} \quad (1)$$

where  $T_{it}$  are the raw temperatures and  $\eta_{it}$  is the idiosyncratic component. The vector of loadings  $\lambda_i$  captures the sensitivity of temperatures at grid cell  $i$  to the aggregate variables

in the vector  $Y_t = [f_t, y_t]'$ . We combine the principal components  $f_t$  of the temperature data with the selected set of economic variables  $y_t$ . This is a simple version of the model in Phillips et al. (2020), where we accommodate spatial dependence of temperatures on common factors. The reduced form model for  $Y_t$  is a VAR of lag order  $p$ :

$$A(L)Y_t = \mu + \epsilon_t, \quad \epsilon_t \sim WN(0, \Sigma) \quad (2)$$

where  $\mu$  is a constant term,  $A(L)$  is a matrix polynomial in the lag operator given by  $A(L) = I - A_1L - \dots - A_pL^p$  and  $\epsilon_t$  is a vector of reduced form white noise errors whose variance-covariance matrix is given by  $\Sigma$ . Treating the principal components  $f_t$  as observed, model (2) is efficiently estimated using OLS for each equation. The lag order is determined using the Akaike information criterion, which yields  $p = 2$ . Higher lag orders do not change our results substantially. The reduced form VAR in (2) is assumed to admit a moving average (MA) representation given by

$$Y_t = C(L)\epsilon_t \quad (3)$$

where  $C(L)$  is obtained by inverting  $A(L)$  and we have dropped the constant as it is immaterial for our identification strategy and the model dynamics.

### 3.2 Identification

To identify economic and temperature shocks we rely on partial identification techniques that have been proposed for the study of business cycle fluctuations. Most environmental models focus on aggregate productivity shocks as drivers of emissions (Annicchiarico et al., 2021). However, the recent contributions in Angeletos et al. (2020) and Forni et al. (2023) have shown that the economy, and by extension also emissions, fluctuates largely because of sources that are not purely related to movements in TFP. Therefore, our analysis is set up to provide evidence on alternative channels for the effect of socio-economic activity on temperatures, beyond RBC-style technology shocks alone. It is most common to distinguish fluctuations of high frequency, business cycle frequency and low frequency. Thus, we adopt the following definition of frequency bands:

**Table 1:** Frequency bands adopted for identification.

Frequency	Low	Business Cycle	High	Full Spectrum
Quarters	$> 40$	$[6, 32]$	$(0, 6]$	$(0, \infty)$

The business cycle frequency is between 6 (1.5 years) and 32 quarters (8 years) as is common in the economic literature (Angeletos et al., 2020). This definition roughly coincides with medium cycles that are observable in climatic data as well. For example, ENSO influences global weather and occurs every 3-5 years and lasts for a year (NOAA, 2023). The higher frequencies coincide with the strongest fluctuations in our temperature data. This component is most similar to the types of weather shocks usually identified in the literature. The low frequency band is where we expect the strongest influence of socio-economic activity to show up, as it contains the slight upward trend in the data that is believed to be caused by human beings. Allowing the medium-cycle band to include a few more years (e.g. to include the 11-year solar cycles) does not affect our results.

The structural MA representation of (3) is given by

$$Y_t = C(L)SHu_t = D(L)Hu_t = K(L)u_t, \quad u_t \sim WN(0, I) \quad (4)$$

where  $SS' = \Sigma$ ,  $HH' = I$ , and  $u_t = H'S^{-1}\epsilon_t$ . Choosing  $S$  to be the lower triangular Cholesky factor of  $\Sigma$ , identification of the structural shocks boils down to pinning down columns of the orthonormal matrix  $H$ . The impulse responses of the economic variables (subindex  $E$ ) and of temperatures (subindex  $T$ ) are then given by

$$IRF_E = D_E(L)H \quad (5)$$

$$IRF_T = \Lambda D(L)H \quad (6)$$

The notation  $C_E(L)$  is shorthand for selecting the rows from each of the matrices in  $C(L)$  which correspond to the entries of  $Y_t$  that belong to economic variables.  $\Lambda$  is the matrix containing the vectors of loadings  $\lambda_i$  for each grid cell.

### 3.2.1 Identification of economic shocks

We identify three economic shocks – a technology shock, an investment shock, and a labor supply shock. These are the three shocks that are proposed as the main business cycle drivers in Justiniano et al. (2010) and Justiniano et al. (2011). To do this we follow the procedure described in Forni et al. (2023) which identifies shocks according to their contribution to the cyclical variances of key variables. Consider the structural representation of equation (4). The cyclical variance-covariance matrix of all variables in  $Y_t$  in the frequency band between  $[\underline{\theta}, \bar{\theta}]$  is given by

$$V(\underline{\theta}, \bar{\theta}) = \int_{\underline{\theta}}^{\bar{\theta}} D(e^{-i\omega})D(e^{i\omega})' d\omega \quad (7)$$

where, for example, in the case of business cycle frequencies  $[\underline{\theta}, \bar{\theta}] = [2\pi/32, 2\pi/6]$  and  $i$  is the imaginary constant  $i = \sqrt{-1}$ . In practice,  $V(\underline{\theta}, \bar{\theta})$  can be obtained by computing the average over a grid of values between  $\underline{\theta}$  and  $\bar{\theta}$  and taking the real part of this average (or computing the inverse Fourier transform of the RHS in (7)). This returns the total variation of all variables in  $Y_t$  in the given frequency band as the diagonal elements of the matrix  $V(\underline{\theta}, \bar{\theta})$ . To identify a particular shock instead, we use a single column  $h$  of the orthonormal matrix  $H$  to obtain

$$\Psi(\underline{\theta}, \bar{\theta}) = \int_{\underline{\theta}}^{\bar{\theta}} D(e^{-i\omega})hh'D(e^{i\omega})' d\omega \quad (8)$$

which is the variation of all variables in the given frequency band stemming from the shock associated with column  $h$ . For our identification strategy, we want to target only specific variables in a given band, so we select the rows of  $D$  that correspond to these variables. Suppose, for example, TFP is ordered second in  $Y_t$ , then  $D_m$  for  $m = 2$  would select the corresponding row. As shown in Forni et al. (2023), this can easily be extended for multiple targets. This is discussed in more detail for the case of temperature shocks where we make use of this technique. We want to find the shock which contributed the majority of fluctuations in the given band to our target variable, so the column  $h$  is identified as:

$$h = \arg \max h' \left( \int_{\underline{\theta}}^{\bar{\theta}} D_m(e^{-i\omega})' D_m(e^{i\omega}) d\omega \right) h, \quad \text{s.t. } h'h = 1 \quad (9)$$

The  $h$  that solves this is the unit-length eigenvector corresponding to the largest eigenvalue of the matrix sandwiched in between  $h'$  and  $h$  in (9) (as shown for the time domain in (Uhlig, 2003)).

We first identify the technology shock as the main driver of low frequency variation in TFP as in Dieppe et al. (2021), which echoes the idea of Gali (1999) to identify technology shocks as the only long-run driver of labor productivity. Maximization does not imply that a single source is responsible for all long-run variation of TFP, but picks out the disturbance that contributes the most to its fluctuations. This method is shown to be robust to interference from other shocks that typically occurs in maximization approaches such as Barsky & Sims (2011). Conditional on the identified technology shock, we then proceed to identifying the investment shock as the main driver of investment over the business cycle. Justiniano et al. (2010) and Justiniano et al. (2011) show that such a shock can be interpreted as a shock to the marginal efficiency of capital, that is, how easily investment is converted to productive capital. The shock typically induces positive co-movement between investment and consumption in both representative and heterogeneous agent models (Auclert et al., 2020). The conditional shock is identified by finding another column of  $H$ , call it  $h_j$ :

$$\begin{aligned} h_j &= \arg \max \quad h'_j \left( \int_{\underline{\theta}}^{\bar{\theta}} D_m(e^{-i\omega})' D_m(e^{i\omega}) d\omega \right) h_j \\ \text{s.t. } & h'_{tech} h_j = 0 \quad \text{and} \quad h'_j h_j = 1 \end{aligned} \tag{10}$$

Finally, the labor supply shock is identified similarly to the TFP shock as the main driver of hours worked in the low frequency, but conditional on both the technology shock and the investment shock. This identification is inspired by Shapiro & Watson (1988) with an analogy to the relationship between Dieppe et al. (2021) and Gali (1999). It is easy to extend the maximization constraints in (10) to pin down this labor supply shock.

### 3.2.2 Identification of temperature shocks

We use a similar method as for the economic shocks to identify temperature shocks. Conditional on the three economic drivers, we extract the maximizers of temperature fluctuations in our data set. Economic theory can inform the identification of economic shocks, whereas there is no clear guideline for the identifying traits of climate related shocks. For example, there is no mutually agreeable sign pattern in output, technology, hours or prices that should ensue from a temperature shock. Nor do zero restrictions using a recursive (Cholesky) or long-run neutrality (Blanchard-Quah) scheme seem appropriate, as these would have to hold at every temperature location in our data set, requiring an impossible number of zero responses to be enforced. Maximizing frequency variations of temperatures has the advantage of being statistically driven rather than theoretically and allows us to target many temperature series simultaneously rather than restricting individual variables. To do this we need to extend the above framework slightly. Call the IRFs of the temperature variables  $\Omega(L) = \Lambda C(L)S$  and collect the columns of  $H$  which identify the economic shocks in  $H_E = [h_{tech}, h_{inv}, h_{lab}]$ . Then the maximization program

is the following:

$$h_{Tj} = \arg \max h'_{Tj} \left( \int_{\theta}^{\bar{\theta}} \Omega_m(e^{-i\omega})' W \Omega_m(e^{i\omega}) d\omega \right) h_{Tj} \quad (11)$$

s.t.  $h'_{Tj} H_E = [0, 0, 0]'$  and  $h'_{Tj} h_{Tj} = 1$

As before,  $h_{Tj}$  is a single column of  $H$  and can be found as the eigenvector of the matrix in the quadratic form in (11). The matrix  $W$  is a weighting matrix which has on its diagonal the square roots of the standard deviations of the  $m$  targeted variables in the frequency band of interest. Given that all our data is measured in degree Celsius this is less of a concern, but is done for completeness.

We do not require the temperature shocks to be orthogonal to each other, only to the economic shocks. This is because the main identifying property these shocks have come from geography. Temperature fluctuations on the US west coast may be driven by other impulses than on the east coast. The targets and bands for identification are chosen as follows:

1. Maximize the low frequency temperature variation everywhere
2. Maximize the full spectrum temperature variation everywhere
3. Maximize the full spectrum temperature variation for the West coast (states that border the Pacific Ocean)
4. Maximize the full spectrum temperature variation for the East Coast (states that border the Atlantic Ocean)
5. Maximize the full spectrum temperature variation for the Gulf of Mexico states (Texas, Louisiana, Mississippi, Alabama, Florida)
6. Maximize the full spectrum temperature variation for non-coastal states
7. Maximize the business-cycle spectrum temperature variation everywhere to capture the ENSO pattern
8. Maximize the high-frequency temperature variation everywhere to capture the weather shock predominantly used in the literature

The choice is motivated by the geographical patterns we observe in the descriptive analysis below, which suggest important temperature commonalities in the Midwest, on the coastal regions, and the Gulf area. Moreover, the maximizer of low frequency temperature movements will likely pick up some non-US socio-economic shocks and the full-spectrum maximizer is the closest to the temperature shock measured in an approach that uses average temperatures, only in this case it is purged of US economic activity.

It is important to point out two properties of the shocks that are identified in our FAVAR framework. First, the shocks induce deviations of temperatures at many geographical locations in the US from their deterministic components. If the deterministic component of temperatures contains any trending behavior, a temperature shock constitutes a deviation from this trend. In that sense, explicitly computing the deviation of

temperatures from some long-term trend and then using these deviations as a shock, as is done in Kahn et al. (2021), for example, is very similar, but skips the identification step that tries to pin point if the deviation comes from human sources or is of natural causes. Second, some climate econometric research stresses the importance of extreme weather events as more suitable measures of temperature shocks (Natoli, 2022). The shocks that we construct are precisely this: they are not predictable from past information about temperatures anywhere in the contiguous US and neither from information about GDP, TFP, investment or hours worked. Whether this information set is sufficient is a difficult question to answer. Moreover, non-linearities or state-dependence may play an important role for the transmission of such shocks, all of which we consider to be important avenues for future research.

## 4 Results

### 4.1 Descriptive results

We begin by summarizing the linkages between the US economy and temperatures through the lens of the model in (1) and (2). As a first exercise we determine the number of shocks which drive US temperatures. In the macroeconomic literature, such shocks are sometimes referred to as *deep shocks* (Forni et al., 2009). We do this by maximizing the full-spectrum fluctuations of all US temperature series without conditioning on other shocks. Notice that this is done on the spectral density matrix in (7) rather than the sample correlation matrix that is used for computation of the principal components. We repeat the same exercise and target the full spectrum of variation in the four economic variables to see how these shocks affect temperatures. The outcomes of this are reported in Tables 2 and 3.

**Table 2:** Cumulative cyclical variances explained by the first six shocks that maximize the full spectrum variation of temperatures at grid-cell level in the US. Rounded to two decimals.

	Low Frequencies						Business Cycles						High Frequencies					
	1	2	3	4	5	6	1	2	3	4	5	6	1	2	3	4	5	6
Avg. Temp.	0.3	0.48	0.58	0.78	0.83	0.87	0.42	0.63	0.78	0.81	0.87	0.92	0.42	0.65	0.77	0.8	0.86	0.92
GDP	0	0.01	0.01	0.07	0.08	0.12	0	0.01	0.01	0.19	0.22	0.27	0.01	0.02	0.02	0.08	0.09	0.12
TFP	0	0.04	0.06	0.23	0.27	0.28	0	0.03	0.07	0.52	0.59	0.6	0.01	0.02	0.04	0.29	0.3	0.31
Hours	0	0.01	0.01	0.08	0.1	0.14	0	0.01	0.02	0.25	0.31	0.36	0.02	0.03	0.05	0.18	0.2	0.22
Investment	0	0.02	0.02	0.04	0.06	0.08	0.01	0.01	0.02	0.13	0.16	0.2	0	0.01	0.03	0.06	0.07	0.09

**Table 3:** Cumulative cyclical variances explained by the first six shocks that maximize the full spectrum variation of GDP, TFP, hours, and investment in the US. Rounded to two decimals.

	Low Frequencies						Business Cycles						High Frequencies					
	1	2	3	4	5	6	1	2	3	4	5	6	1	2	3	4	5	6
Avg. Temp.	0.03	0.22	0.31	0.33	0.4	0.47	0.01	0.02	0.05	0.06	0.14	0.24	0.01	0.02	0.03	0.04	0.1	0.2
GDP	0.93	0.96	1	1	1	1	0.71	0.84	0.91	0.99	0.99	0.99	0.78	0.83	0.87	0.93	0.93	0.97
TFP	0.57	0.96	1	1	1	1	0.17	0.83	0.92	0.98	1	1	0.42	0.78	0.84	0.91	0.95	0.97
Hours	0.78	0.98	0.99	1	1	1	0.43	0.96	0.96	0.99	1	1	0.34	0.85	0.88	0.94	0.96	0.98
Investment	0.88	0.94	0.97	1	1	1	0.53	0.75	0.76	0.99	1	1	0.44	0.54	0.55	0.9	0.93	0.99

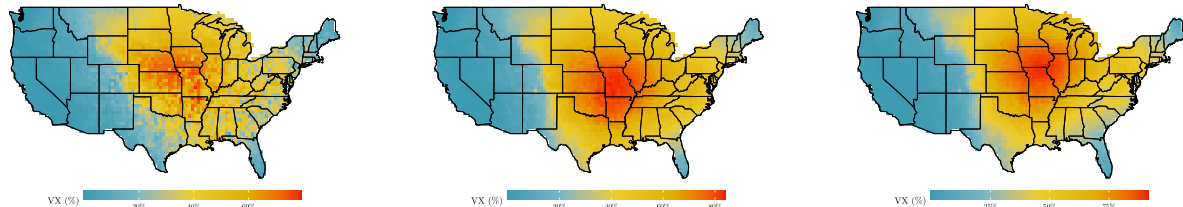
Two important new findings emerge from these tables. First, the common variation in US temperatures requires at least five shocks to reach more than 80% explained cyclical

variance at all frequencies. After the fifth shock, the improvement in explained variance in any of the three bands of interest from adding another shock is below 5%. This number constitutes a lower bound for the actual number of exogenous temperature drivers, as the shocks here are not structurally identified, other than being mutually orthogonal variance maximizers. Based on this result, reducing the effects of temperatures on economic aggregates to a single variable such as a (weighted) average, as is frequently done in the literature, necessarily tells a partial story of global wide-spread temperature change.

Second, there is a connection between temperature and economic variation, mostly through TFP. The fourth temperature variance maximizer is responsible for a sizable increase in the share of TFP variation at all frequencies, particularly at the medium part of the spectrum. The space spanned by the five shocks appears to admit room for both natural and economic shocks. This is confirmed when targeting the four economic variables instead of temperatures. The results of this reverse exercise are presented in Table 3. We observe that, in line with the literature (e.g. Forni et al. (2023)), two shocks appear sufficient to capture a large share of the cyclical variation in key economic aggregates. In the low frequency and business cycle bands, hours, investment, and GDP are largely driven by the same shock, yet TFP is not. This echos the findings of Angeletos et al. (2020) who also demonstrate a disconnection between TFP and business cycle fluctuations of GDP. Crucially, we see that the second shock, which substantially improves the explained cyclical variance of long-run TFP is responsible for a sizable increase in the explained variance of low frequency US temperatures. Since it does not affect higher frequency movements, we take this as preliminary evidence for the shock being of economic origin rather than natural.

While these descriptive results report only the variation in average US temperatures, our model allows us to disaggregate the effects down to the grid cell level. This is presented in Figure 4 for the five temperature variance maximizers and in Figure 5 for the first four economic maximizers. As is visible from the spatial distribution of explained variances in Figure 4, the first shock is unsurprisingly strongly related with the first principal component of the temperature data – it is centered in the Midwest region of the US. The second shock is mostly responsible for variation on the west coast and the third shock picks up signals more strongly near the Canadian and Mexican borders. This result is partly due to the imposition of orthogonality of the shocks and commonly observed in the study of EOFs (Hannachi et al., 2007). For the economic maximizers, on the other hand, we note that the primary driver of low frequency variation hardly has any impact on US temperatures. Effects are stronger for the second, third and fourth shocks that are more related to TFP and investment. We take the following lessons from this descriptive section: first, it seems reasonable to distinguish shocks by geographic criteria, such as a heartland and a coastal shock, with a distinction between west and east coast also warranted. Second, imposing orthogonality for these shocks may create artificial geographical patterns. We therefore choose to condition only on the economic shocks and treat the temperature shocks one-by-one, without imposing that they themselves be mutually orthogonal. Third, there is a clear connection between the economy and temperatures. However, the descriptive exercise does not permit us to tell apart the respective source of the fluctuation, so we proceed with the proposed identification scheme next.

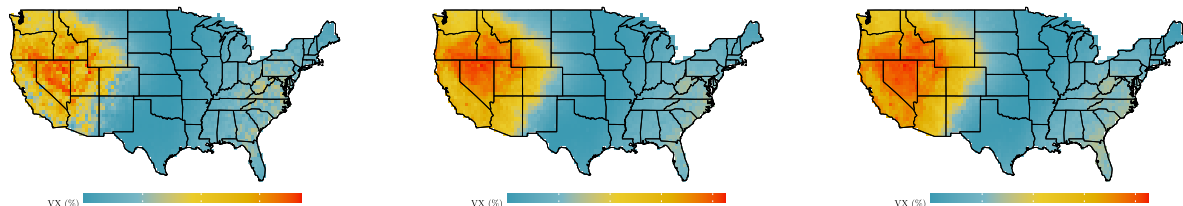
**Figure 4:** Cyclical temperature variation explained in each grid cell in the US from the first five shocks which maximize temperature variation over the full frequency spectrum.



(a) Shock 1 at LF

(b) Shock 1 at BC

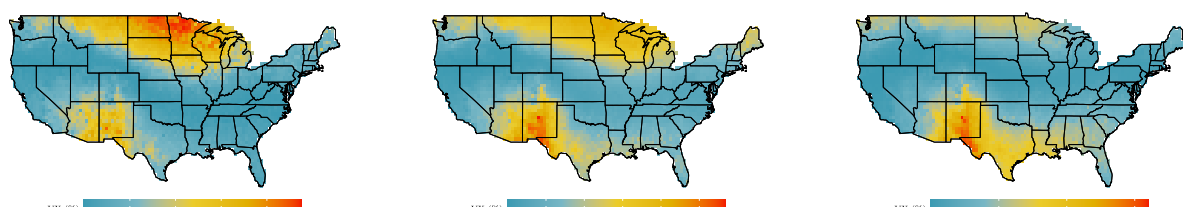
(c) Shock 1 at HF



(d) Shock 2 at LF

(e) Shock 2 at BC

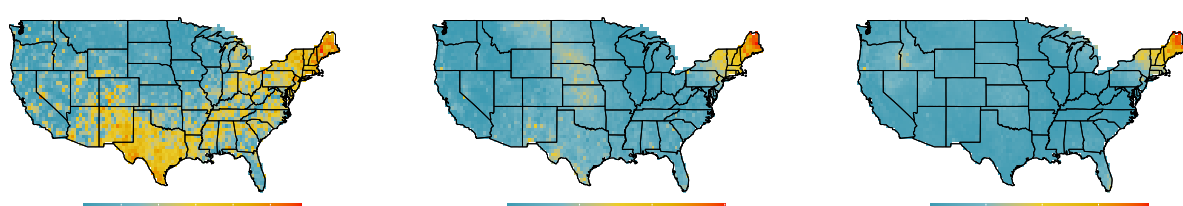
(f) Shock 2 at HF



(g) Shock 3 at LF

(h) Shock 3 at BC

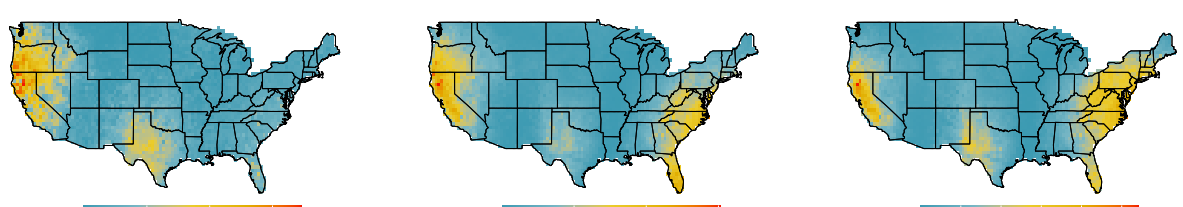
(i) Shock 3 at HF



(j) Shock 4 at LF

(k) Shock 4 at BC

(l) Shock 4 at HF

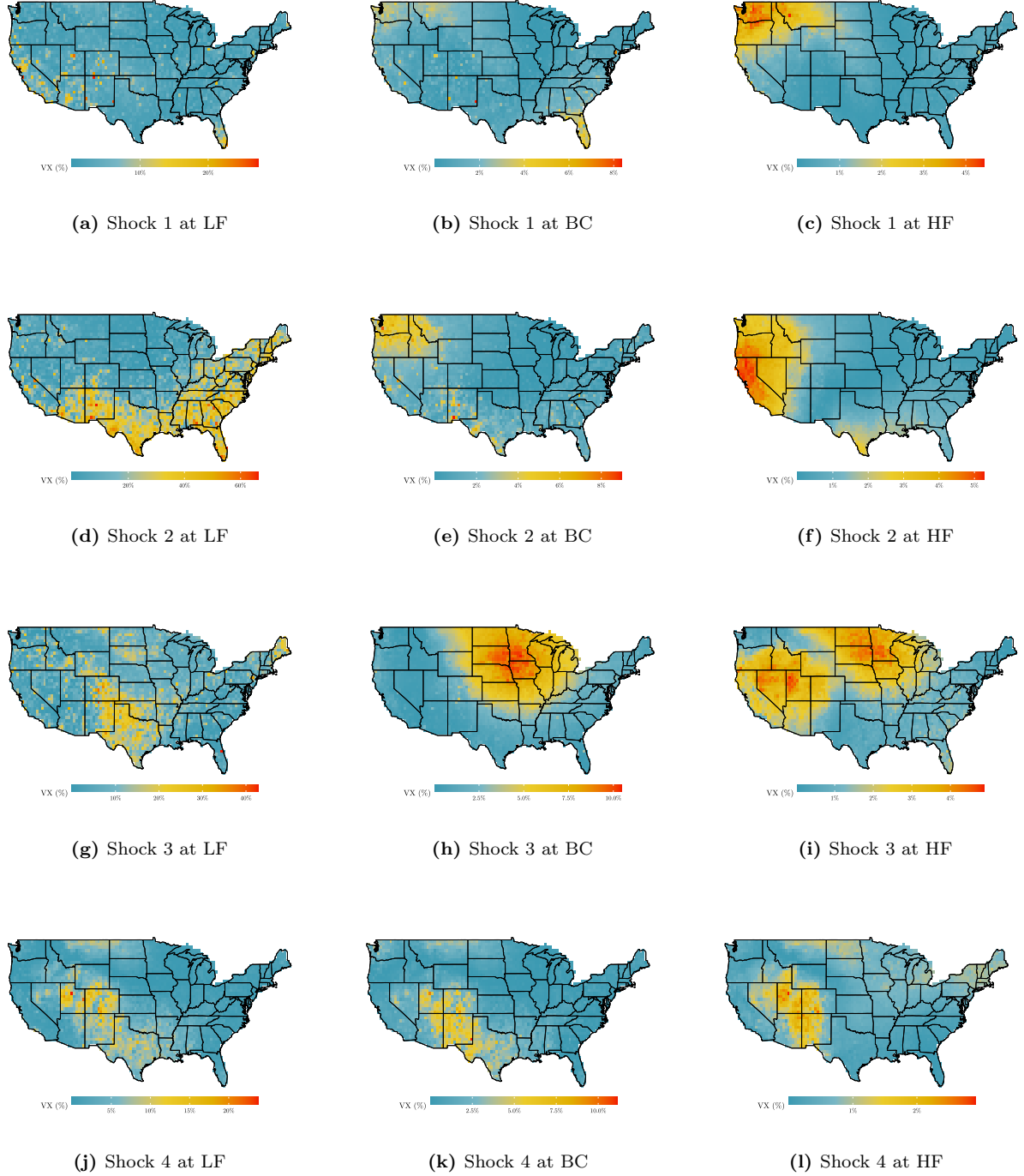


(m) Shock 5 at LF

(n) Shock 5 at BC

(o) Shock 5 at HF

**Figure 5:** Cyclical temperature variation explained in each grid cell in the US from the first four shocks which maximize the economic variables' variation over the full frequency spectrum.



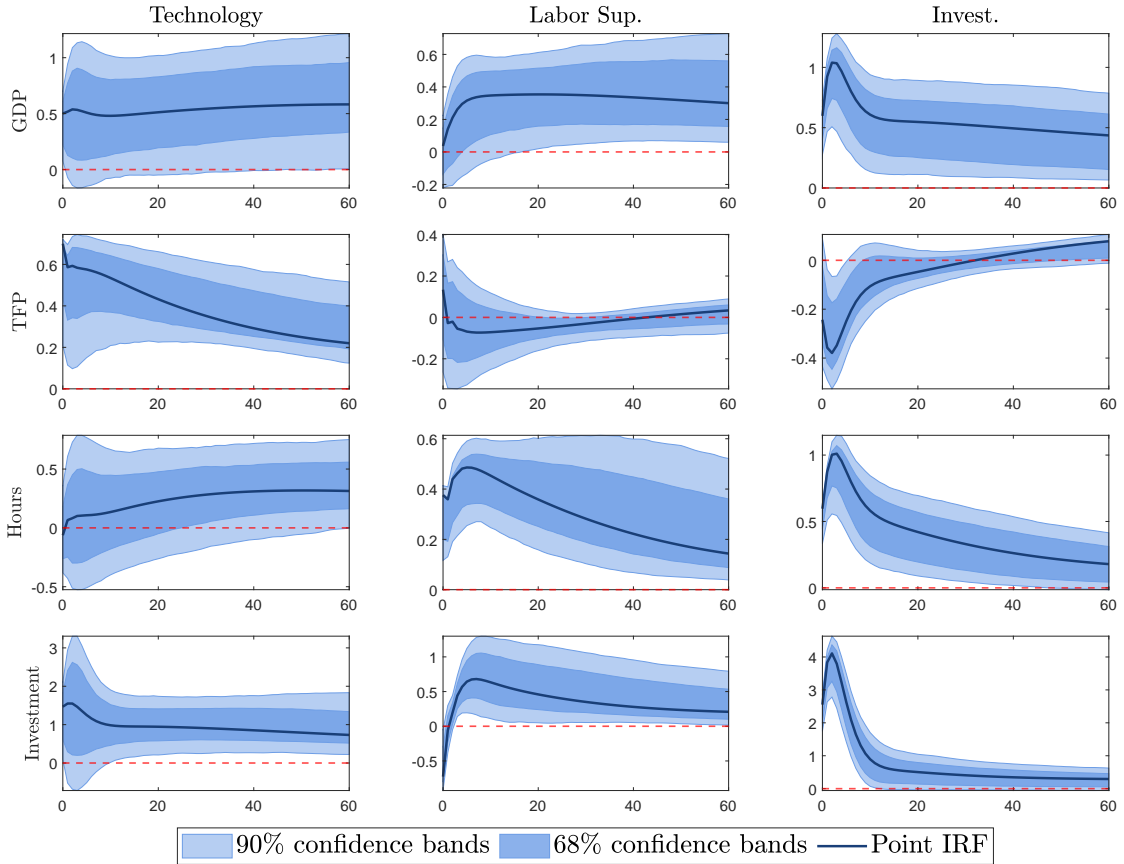
## 4.2 Semi-structural results

### 4.2.1 Economic shocks

We begin by discussing the effects of the economic shocks on the economic variables. This is done to confirm that our identification procedure is indeed successful in selecting technology, labor supply, and investment related shocks as described in the macroeconomic

literature. The impulse response functions for this are reported in Figure 6.

**Figure 6:** Impulse response functions for the three structural economic shocks. Shaded areas are bootstrapped 68% and 90% confidence bands.



First, the technology shock leads to an immediate increase in TFP which is accompanied by an expansion of real GDP of around 0.4%. Hours initially decline (although this is statistically insignificant) and investment increases. These results are very similar to those found in Dieppe et al. (2021), who use labor productivity in a spectral identification exercise with a different VAR specification. Second, the labor supply shock leads to a slowly-building increase in output of around 0.3%, a mildly hump-shaped response of hours after an initial increase and an initial reduction in investment which is replaced by labor as an input to production. The TFP response is almost entirely insignificant, which is partially a result of conditioning on the technology shock. The slow-building GDP response is consistent with other studies that identify labor supply shocks such as Foroni et al. (2018) (for the US) and Peersman & Straub (2009) (for the euro area). The responses of hours and GDP are in line with the paper of Shapiro & Watson (1988), which we have used as motivation for the identification strategy. Lastly, the investment shock creates hump-shaped expansions in investment, hours and GDP and a hump-shaped decline in TFP. These responses are in line with the motivating paper of Justiniano et al. (2011). The decrease in TFP is also observed in Ben Zeev & Khan (2015) (although in their paper the response is insignificantly different from zero) for investment-specific technology shocks. More inputs are used to produce only slightly more output, thus productivity must fall. We take these results as evidence that our proposed identification strategy

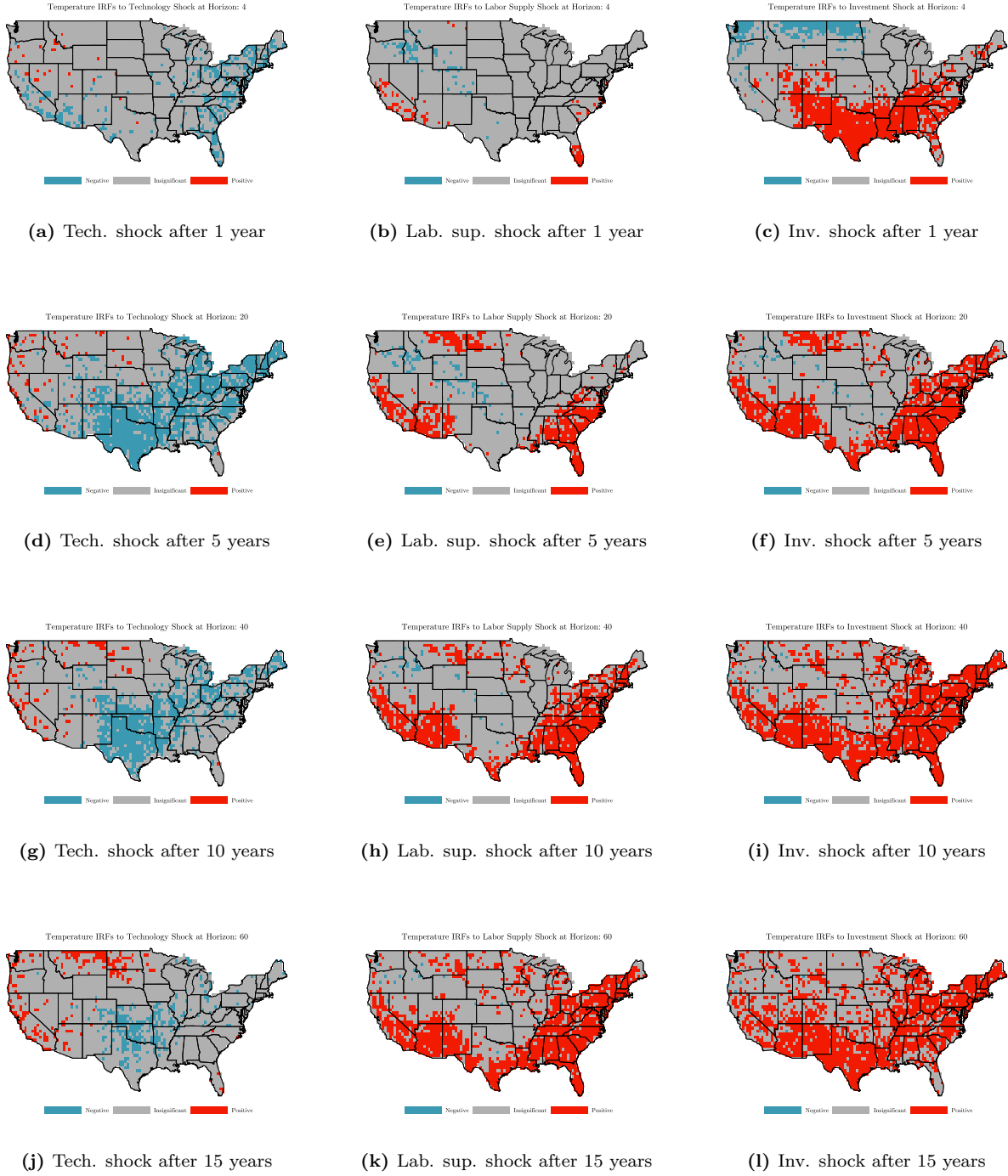
can indeed correctly pick out empirically valid impulse responses in a joint identification framework, even though the identification approach is entirely built on spectral identification and does not exactly copy the approaches in the originally proposed papers.

Next, we describe the responses of US temperatures to the three expansionary economic shocks, a key result of this chapter. It is important to note that the impact reactions (near impulse response horizon  $h = 0$ ) of temperatures across the US to the shocks are difficult to measure accurately due to the high volatility of the temperature time series' as opposed to the macroeconomic aggregates. We therefore prefer to not interpret temperature responses to economic shocks near the impact. The graphs in Figure 7 show the following picture: the technology shock has a cooling effect on temperatures in the east and the south of the US. Importantly, as the impulse horizon increases, the effect dissipates almost everywhere, which suggests that eventually, cooling and warming offset each other. The effect is persistently significant at the 68% confidence level even after 10 years. The investment shock leads to increases in temperatures almost in the entire US after 10 years, after initially dominating in California, Arizona, near the Canadian border, and in the east. Finally, a similar pattern emerges for the labor supply shock, although the initial temperature responses are less pronounced compared to the investment and technology shocks. As far as the magnitudes of the responses are concerned, they range between  $-0.03$  and  $0.01$   $^{\circ}\text{C}$  (technology shock),  $-0.01$  and  $0.02$   $^{\circ}\text{C}$  (labor supply shock) and  $-0.01$  and  $0.02$   $^{\circ}\text{C}$  (investment shock).<sup>2</sup>

---

<sup>2</sup>These values are computed across all horizons and grid cells as a single standard deviation around the mean response for each of the three shocks.

**Figure 7:** Grid cell temperature IRFs at given horizons in response to the three economic shocks.



Next, we report the relative importance of each of the three economic shocks in explaining average temperature movements, as well as the fluctuations of our economic variables at low, business cycle, and high frequencies.

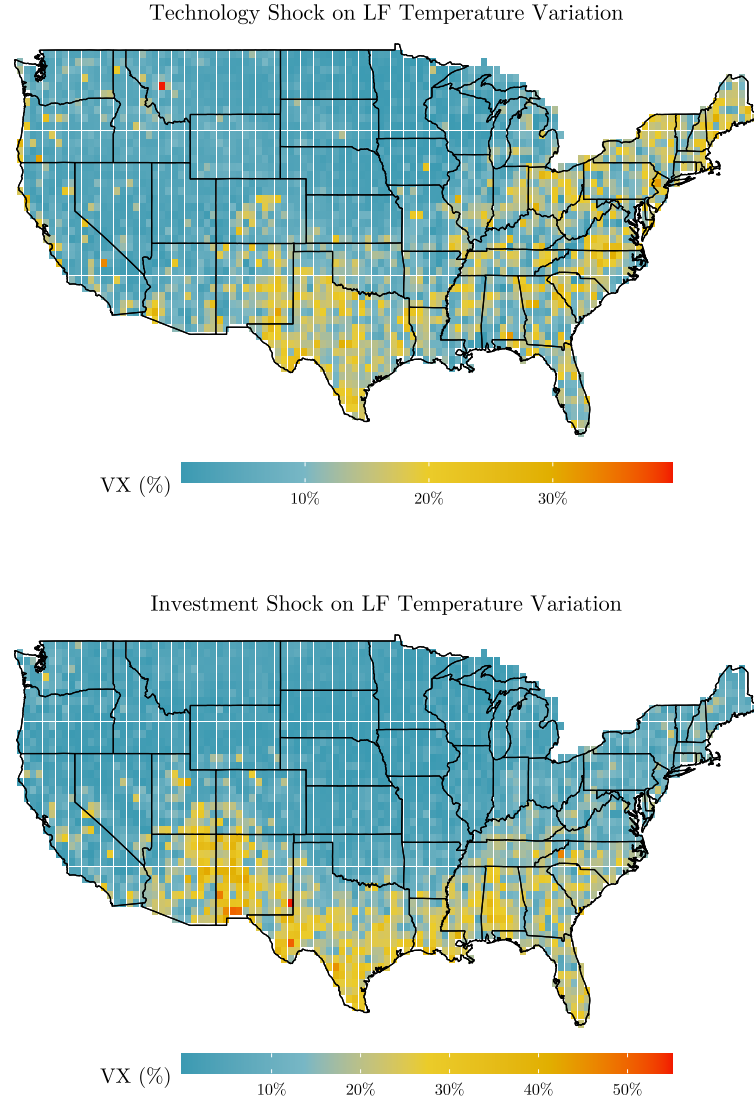
**Table 4:** Individual cyclical variances explained by the three identified economic shocks over the three frequency bands. Numbers in parentheses are the 90% confidence bands associated with the percentage above. Rounded to two decimals.

	Low Frequencies			Business Cycles			High Frequencies				
	Tech.	Lab.	Sup.	Invest.	Tech.	Lab.	Sup.	Invest.	Tech.	Lab.	Sup.
Avg. Temp.	0.1 (0.04,0.36)	0.04 (0.04,0.19)	0.11 (0.05,0.22)	0.01 (0.01,0.06)	0.01 (0.01,0.06)	0.01 (0.02,0.07)	0.01 (0.02,0.07)	0.01 (0.01,0.05)	0.01 (0.01,0.05)	0.01 (0.01,0.05)	0 (0.03)
GDP	0.46 (0.04,0.93)	0.13 (0.01,0.47)	0.34 (0.02,0.58)	0.24 (0.04,0.75)	0.05 (0.01,0.21)	0.58 (0.13,0.73)	0.46 (0.11,0.79)	0.04 (0.01,0.26)	0.46 (0.06,0.54)	0.04 (0.01,0.26)	0.36 (0.02,0.21)
TFP	0.84 (0.62,0.99)	0.02 (0.01,0.16)	0.08 (0.01,0.15)	0.57 (0.14,0.83)	0.02 (0.01,0.27)	0.28 (0.04,0.46)	0.7 (0.19,0.72)	0.07 (0.01,0.29)	0.07 (0.02,0.21)	0.07 (0.01,0.29)	0.09 (0.02,0.21)
Hours	0.32 (0.06,0.83)	0.24 (0.07,0.5)	0.44 (0.04,0.65)	0.04 (0.02,0.53)	0.14 (0.03,0.21)	0.79 (0.26,0.82)	0.13 (0.07,0.59)	0.24 (0.04,0.29)	0.13 (0.14,0.56)	0.24 (0.04,0.29)	0.54 (0.14,0.56)
Investment	0.52 (0.11,0.89)	0.08 (0.01,0.33)	0.39 (0.06,0.64)	0.1 (0.02,0.51)	0.03 (0.01,0.07)	0.85 (0.42,0.92)	0.21 (0.06,0.42)	0.11 (0.01,0.16)	0.21 (0.26,0.66)	0.11 (0.01,0.16)	0.56 (0.26,0.66)

Taken together the three economic shocks explain around 25% of the low frequency movement of temperatures. Technology and investment shocks contribute the most (10% and 11% respectively), labor supply shocks contribute less (4%). We conclude from this that a non-negligible share of the trend- and long-cycle component of temperatures is caused by anthropological activity in the United States. The economic shocks are not important sources of average short-term temperature fluctuations, which we take as evidence for such fluctuations as being mostly of natural or non-US causes. The three shocks also appear to be reasonable choices to explain business cycle fluctuations in the economy. Together they account for 87% of the BC variation in GDP, 87% of the variation in TFP, 97% of the variation in hours, and 89% of the variation in investment.

The spatial distribution of explained variances of the shocks is presented in Figure 8. Given that there is hardly any variance arising at medium and short frequencies, we report this only for the low frequency and only for the technology and the investment shock. Patches of relevant fluctuations are observable in both cases. For the technology shock, variances explained are around 35% in the east and in the south, particularly in Texas. For the investment and the labor supply shocks, the patterns emerge predominantly in the south and in the corridor across Colorado, Wyoming, and Idaho, for which the labor supply shock was cooling. Explained variances for the investment shock are locally larger than 40% in some areas in the south.

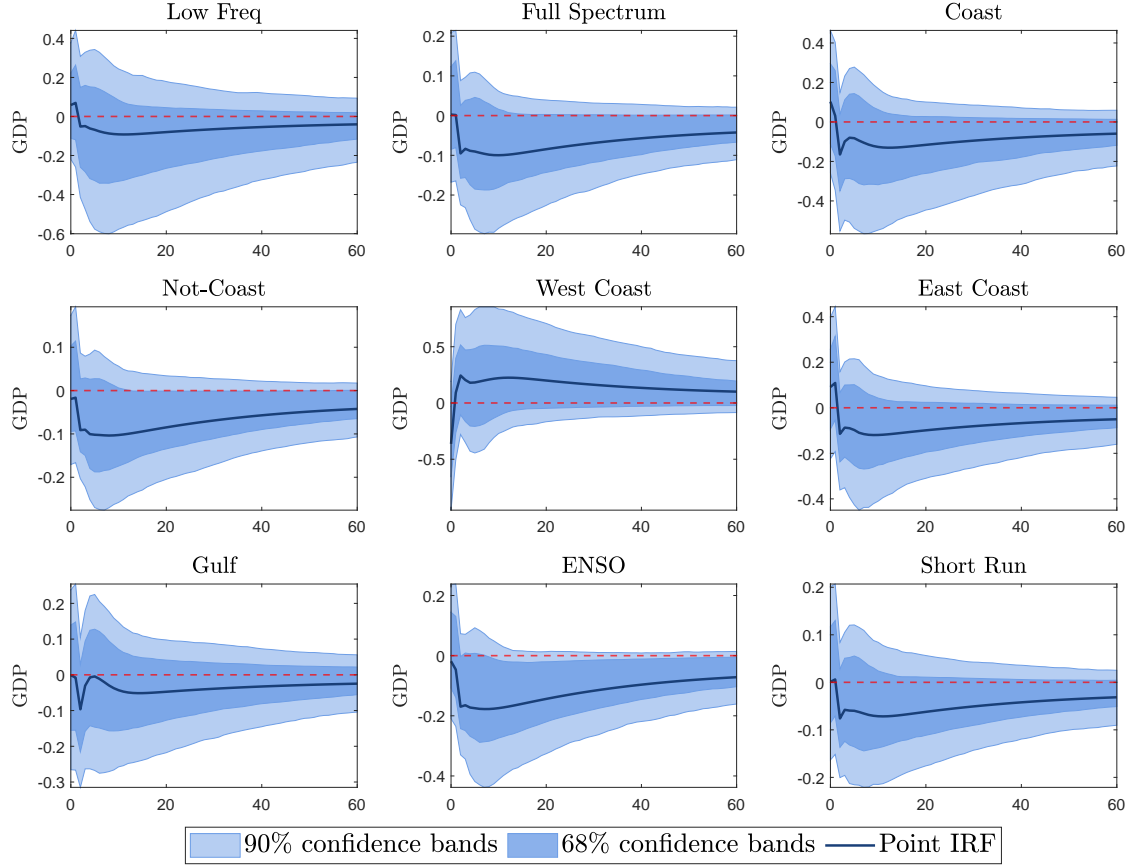
**Figure 8:** Grid cell level cyclical variation explained at low low frequencies from the economic shocks.



#### 4.2.2 Temperature shocks

Next, we turn to the effects of the temperature shocks that are identified as described in section 3. For ease of interpretation we have normalized all shocks such that the impact response in average temperatures is scaled to 1 degree Celsius, as is customary. We are primarily concerned with the effect of temperature changes on GDP as this is the outcome typically used in the literature as a gauge for climate damages. Figure 9 summarizes the resulting IRFs.

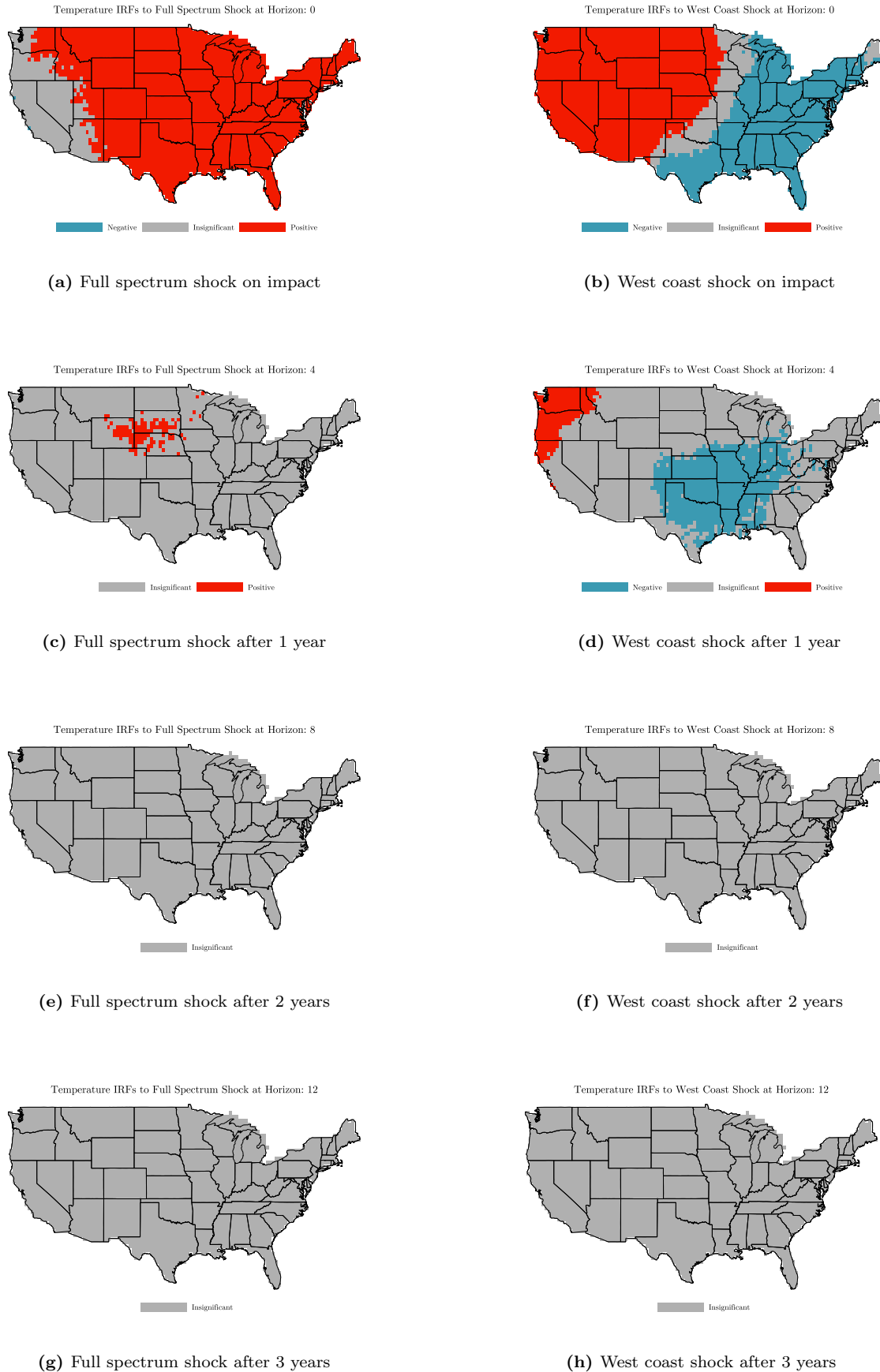
**Figure 9:** Impulse response functions for the different temperature shocks. Shaded areas are bootstrapped 68% and 90% confidence bands.



All of the identified shocks lead to small and persistent GDP contractions between 0.1% and 0.2% except for the shock that hits primarily the West coast of the US. The confidence bands are always very close to the zero line. This result is consistent with the majority of the literature, which finds substantial uncertainty involved in the estimates of temperature shocks in the US, see for example Newell et al. (2021) and Nath et al. (2023), who find nearly zero effect for countries with an average temperature around 13 degrees Celsius such as the US. Negative effects of temperature shocks in the range of 0.1% are also found in Natoli (2023) (although using an instrumental variable approach) and slightly more negative impacts are documented in Colacito et al. (2019), while Dell et al. (2012) found insignificant effects of temperatures on rich countries' output. The results that these papers obtain are consistent with the shock in our set, which maximizes temperature variation in the entire US over all frequency bands. However, we can go beyond this based on our conclusion that more than one shock is required to capture US temperature variation. In fact, without imposing orthogonality for this exercise, the West coast shock is only 2% correlated with the low-frequency maximizer, 3% with the full spectrum maximizer, and a relatively low 33% with the East coast shock. Interestingly, it produces a comparatively sizable expansion in aggregate GDP (although this is statistically insignificant). This effect would either be lost entirely or mixed into average results obtained through the usual econometric techniques. As Table 4 suggests, the share of variation in the economic variables from temperature movements are very small, which is why we choose not to report them here.

For illustration of the spatial distribution of impulse responses, we focus on the full spectrum maximizer for temperatures everywhere and the west coast shock. These two shows are only 3% correlated, without the imposition of orthogonality. Figure 10 shows the signs of the responses. Clearly, the full spectrum maximizer without geographical constraints raises temperatures everywhere except for the west coast. The shock which drives temperatures up on the west coast, simultaneously decreases them in the east. Due to the scaling of the average temperature to equal 1°C, the positive responses outweigh the negative ones. Both of these shocks are quantitatively important for temperature variations (38% and 16% on average respectively over all frequency bands). Importantly, we find no evidence of significant persistence in either of the temperature shocks considered here. After around three years, all effects on temperatures turn insignificant.

**Figure 10:** Grid cell temperature IRFs at given horizons in response to the full spectrum and the west coast temperature shocks.



To summarize the semi-structural results, we see that economic sources, especially technology and investment shocks, are locally important drivers of temperature variations. They lead to noticeable decreases (technology) and increases (investment, labor supply) in temperatures that persist for many years and are noticeable even relatively shortly after the initial shock. Treating temperatures as unaffected by anthropological forces even in the short run can thus lead to confounding causal effects, especially when annual data is used as is customary in the literature. Moreover, it is important to distinguish the effects of temperature shocks on aggregate GDP by the geographical location of the epicentre of the shock. If the west coast is predominantly affected, GDP may be unaffected or even increase, while shocks in the rest of the country lead to small contractions. This is important for assessing the damages of temperature warming which are fed into models used for policy decisions.

## 5 Discussion

### 5.1 The effects of economic shocks on temperatures

The documented effects of the three economic shocks on temperatures across the US warrant closer inspection. The connection between economic activity and temperatures runs through the emission and storage of climate-active gases. Magnus et al. (2011) decompose the temperature effect of anthropogenic gas emissions into warming – through the emission of GHGs, most prominently CO<sub>2</sub> – and cooling – through aerosol emissions, most prominently SO<sub>2</sub>. CO<sub>2</sub> is a long-lived, well-mixing gas, which spreads through the Earth’s atmosphere over time, while SO<sub>2</sub> produces quick, but more short-lived localized cooling by reflecting incoming solar radiation. There is increasing evidence from the natural sciences that emission impulses can lead to temperature effects within a very short time span. Notably, Ricke & Caldeira (2014) and Zickfeld & Herrington (2015) suggest that CO<sub>2</sub> emission impulses can lead to significant warming relatively quickly – 93% of the peak warming effects materialize after 10-15 years following an emission impulse in their experiments, even taking potential non-linearities into account. Such horizons are well within the customary projection range for FAVAR models. Complementary to this, Joos et al. (2013) calculate average surface-temperature responses to CO<sub>2</sub> emission impulses and find positive reactions contemporary with the initial impulse. Methane is another powerful GHGs that develops much of its effects over a short horizon (Mar et al., 2022). Therefore, our finding of quick temperature changes in the US after economic shocks is in line with results found in climatology research. Nevertheless, we want to emphasize that the very long run where GHG effects are still active may be less precisely estimated in our model.

Technology shocks induce cooling in parts of the US east and south. This suggests that the solar radiation effect from aerosol emissions outweighs the heating effect from GHG emissions at these locations, especially in the short run. We investigate this hypothesis further by running the following analysis: to the VAR consisting of GDP, TFP, investment and hours worked we add time series for GHGs and SO<sub>2</sub> emissions in the US for the same sample we have used in our previous analysis. Unfortunately, emissions are available only at yearly frequency. The data for GHGs are retrieved from <https://ourworldindata.org/greenhouse-gas-emissions> and are

based on Jones et al. (2023), the data for SO<sub>2</sub> are from Smith et al. (2011) until 1990 and from then on from the EPA (<https://www.epa.gov/air-emissions-inventories/air-pollutant-emissions-trends-data>). We estimate the VAR with a single lag and identify a technology shock and an investment shock in exactly the same fashion as before, using frequency domain techniques.

**Figure 11:** Impulse response functions of log emissions to technology and investment shocks in the yearly VAR(1) for only economic variables. Identification in the frequency domain adapted to yearly measurements.

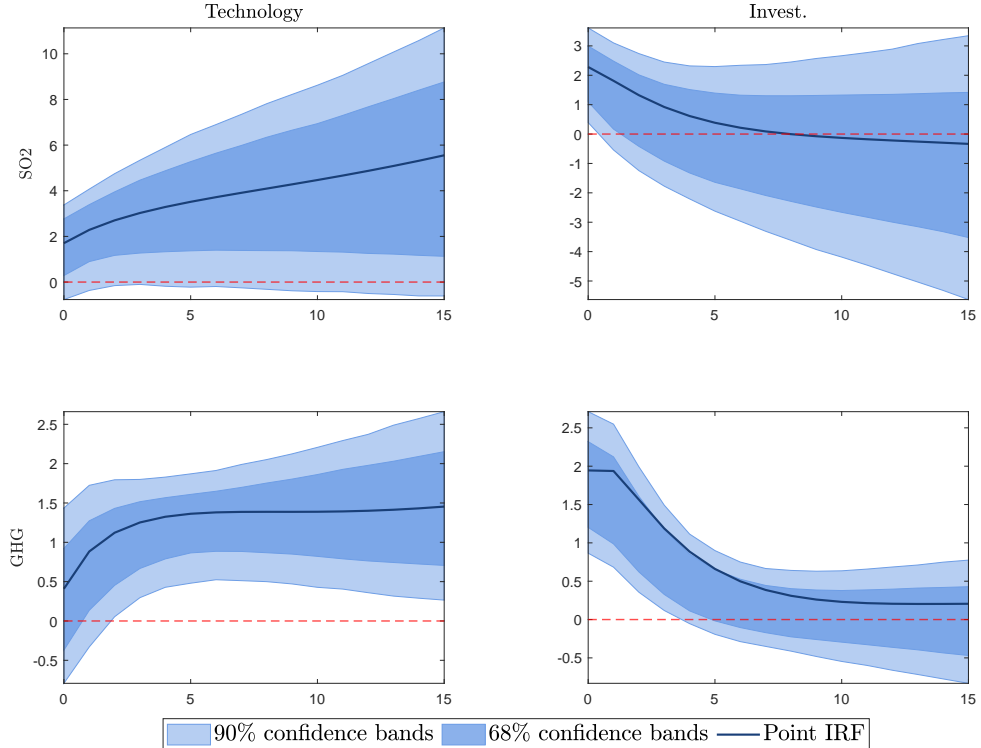
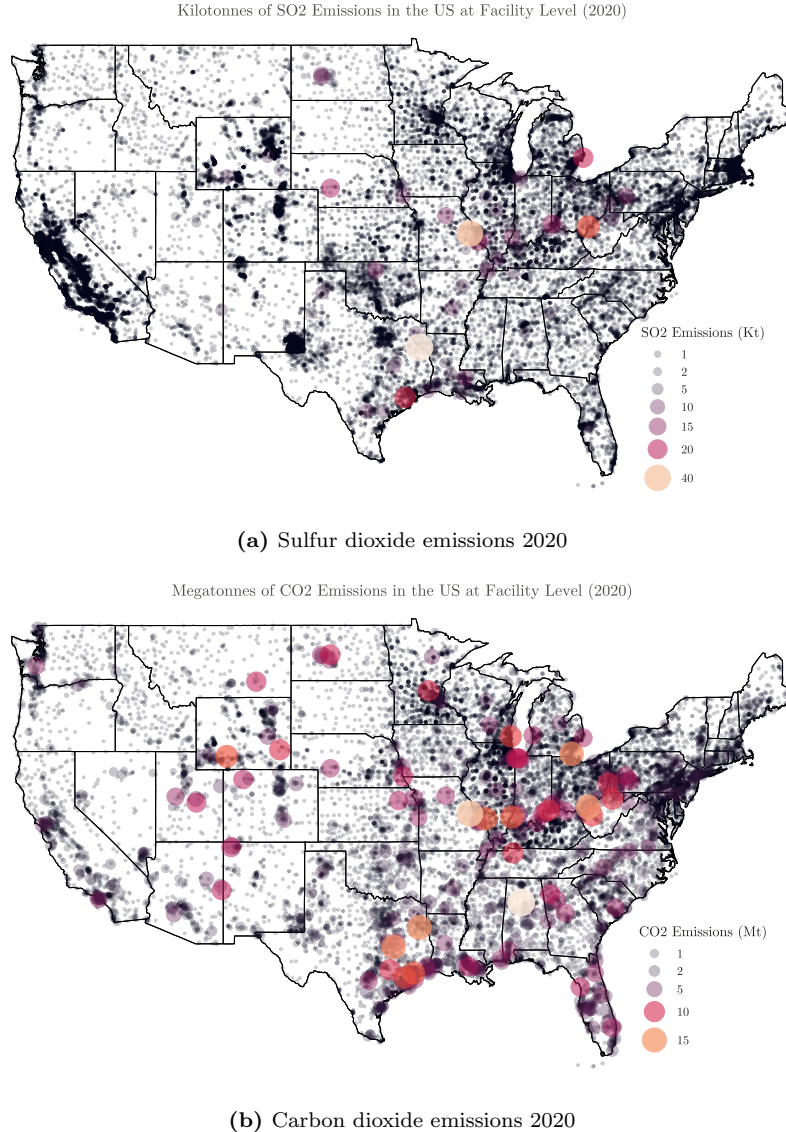


Figure 11 shows the responses of SO<sub>2</sub> and GHG emissions to the two expansionary shocks. The IRFs for the other economic variables are in line with the quarterly exercise and are therefore not reported again. The permanent shock to TFP also leads to permanent increases in both SO<sub>2</sub> and GHG emissions, but the increase in SO<sub>2</sub> emissions is in the area of 2% initially and up to 6% after 15 years, while GHG emissions increase only between 0.5% on impact and slightly below 1.5% in the long run. We take this as evidence that what we pick up in the quarterly FAVAR is cooling from increased aerosol emissions. This also speaks to the localized effects in the south-east of the country which we comment on more below. Importantly, as suggested in Magnus et al. (2011), SO<sub>2</sub> is itself short-lived and so in spite of the sustained increase in SO<sub>2</sub> emissions, the cumulative warming effect from GHGs eventually neutralizes the cooling from aerosols in our quarterly FAVAR, which is why as the IRF horizon increases, the cooling effects disappear or even turn to warming. For the investment shock, on the other hand, we see impulses in both SO<sub>2</sub> and GHGs of equal magnitude, but the SO<sub>2</sub> impulse is only mildly significant for about one year before emissions (insignificantly) reduce. GHG emissions are strongly increased and persist for a longer period, which is why the cooling effect here dissipates

fast and is dominated by the warming effect from GHGs throughout the horizon in the quarterly FAVAR. This also explains, why the temperature changes after the investment shock are observed across almost the entire country and remain significant even after 15 years – there is no sustained counteracting cooling effect.

Curiously, the geographical pattern of temperature changes after a technology shock in Figure 8 roughly coincides with the location of important parts of the American energy producing, manufacturing and natural resource processing industries. Figure 12 shows that these areas are also centres of CO<sub>2</sub> and SO<sub>2</sub> emissions. Conley et al. (2018) study the responses of temperatures to the hypothetical removal of all US based SO<sub>2</sub> emissions and document a very similar geographical pattern (evidently with inverted signs as they consider SO<sub>2</sub> removal, instead of emission). Based on this observation, we are confident that our economic shocks lead to temperature-altering emissions in the parts of the country where these should be expected to occur. Moreover, given the localized nature of aerosol-related cooling, we take this spatial pattern as evidence that the channel we pick up for our technology shock is indeed dominated by SO<sub>2</sub> emissions.

**Figure 12:** SO<sub>2</sub> and CO<sub>2</sub> emissions are computed from EPA’s NEI 2020 data set for site-specific emissions (data retrievable from <https://www.epa.gov/air-emissions-inventories/2020-national-emissions-inventory-nei-data>). These include emissions from fossil fuel combustion, industrial processes and biomass (e.g. wildfires), but exclude *onroad* emissions.



## 5.2 The effects of temperature shocks on GDP

Next, we turn to the discussion of the different effects of west coast centered temperature shocks and the other temperature shocks we have identified. We focus on the full spectrum maximizer as a representative of the other shocks and recall that both shocks lead to a one centigrade increase in average US temperatures, but the GDP responses present opposite signs. Our reasoning for this finding is based on previous results in the literature. First, consider sector level responses. Increases in temperatures have been shown to reduce output in almost every industry, especially in agriculture and construction (Colacito et al., 2019). The temperature increase that follows the full spectrum shock affects almost the entire US and thus essentially all industries (a notable exception being California), thus depressing also aggregate GDP. Conversely, the west coast shock leads to increased

temperatures on the west coast, but is accompanied in the data by lower temperatures in the east. In our linear model, decreasing temperatures should be beneficial for output in those states. The heating in the west does not appear to offset this positive effect.

Second, we turn to geographical differences. Hsiang et al. (2017) provide estimates of the projected spatial distribution of climate effects for the US. They calculate a gain in agriculture from increased temperatures in the north-west of the country and project overall total damages to concentrate in the south-east of the country, whereas the north-western states experience positive effects from warming. The largest damages from temperature increases go through excess mortality in the densely-populated east and the already warmer south of the US in their study, also reported by Carleton et al. (2022). Therefore, the warming in the west and cooling in the east we document after the west coast shock should benefit the western industries and lead to fewer deaths in the east, which sums to a net positive effect for aggregate GDP. The full spectrum shock, on the other hand, does not produce the warming gains in the north-west but leads to warming in the areas where excess mortality has been shown to be of high importance in the transmission of temperatures to GDP.

In light of these arguments, we carry out the following exercise to better understand how the shocks impact state-level income. We expect the full spectrum shock to be damaging almost everywhere and the west coast shock to be expansionary, at least in the eastern states, but potentially also in the west. To do this, we run the following local projections (Jordà, 2005) for each state in the contiguous US individually:

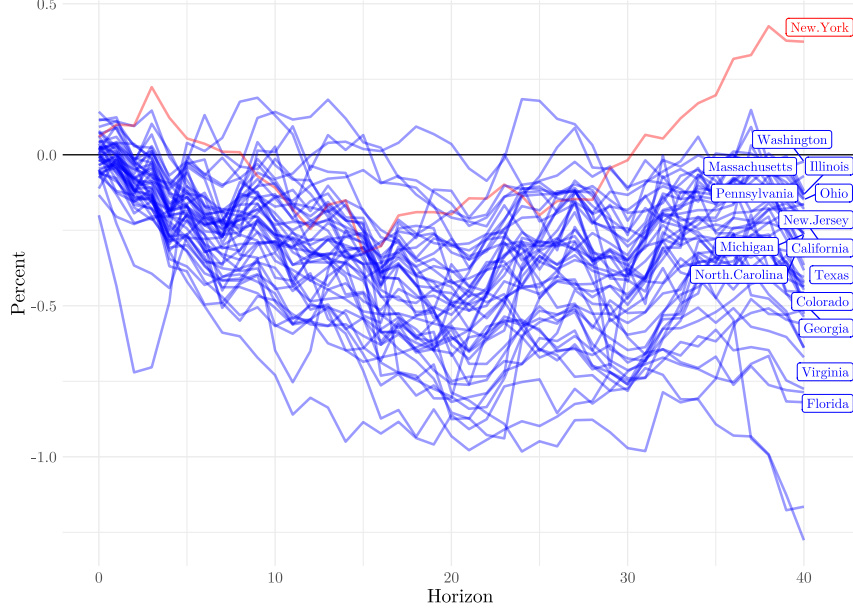
$$y_{t+h} = \mu_h + \beta_h \hat{s}_t + \gamma_h(L)y_{t-1} + \epsilon_{t+h}, \quad \text{for } h = 1, 2, \dots, 40 \quad (12)$$

where  $y_{t+h}$  is the log of quarterly real personal income<sup>3</sup>,  $\mu_h$  is a constant,  $\hat{s}_t$  is alternatively the unit variance full spectrum or west coast shock estimated in the FAVAR,  $\gamma_h(L)$  is a lag-polynomial of order two as in the FAVAR and  $\epsilon_{t+h}$  is a forecast error. The coefficient  $\beta_h$  measures the response to the shock of interest at each horizon  $h$ .

---

<sup>3</sup>Personal income data at the state level at quarterly frequency is collected from BEA table SQINC4 and deflated using the GDP deflator and alternatively the CPI. The sample spans Q1:1948 - Q4:2017.

**Figure 13:** Impulse responses to the full spectrum and the west coast temperature shocks identified in the FAVAR. IRFs are obtained by means of a local projection of real personal income at the state level onto its own lags and the identified unit variance shock. The states with name tags are the largest 15 states by GDP. Blue lines indicate negative responses after 40 quarters. Red lines indicate positive responses after 40 quarters.



(a) Full spectrum shock on real personal income



(b) West coast shock on real personal income

Figure 13 shows that the full spectrum temperature shock indeed decreases income in nearly all states, except for New York, which nonetheless experiences reductions in income for most of the horizon. The west coast shock, on the other hand, produces mixed IRFs. The majority of economically large states (by share of national GDP) experience income increases, except for Colorado, Florida and Texas, where the losses are relatively small. Big west coast economies such as California and Washington see long-run benefits

from the shock, although these are small in magnitude. We take the evidence from this auxiliary model as supportive of the idea that temperature increases, in general, are detrimental for output, possibly by increasing mortality or lowering productivity. However, we caution that a measured increase of average US temperatures of one degree Celsius can come in different shapes, that produce different dynamics at the state level which then translate into different aggregate responses. We believe that our two example shocks are good representations of actual co-movement in temperatures experienced in the US. Any exercise focusing on the simple average temperature, which is similar to the full spectrum maximizer, will likely miss the effects induced by the west coast shock and may lead to incomplete conclusions for damage functions and policy implications.

### 5.3 Counterfactual

We have shown that temperatures in the US react significantly to economic shocks and that temperature shocks, which are orthogonal to these economic shocks predominantly lead to small or insignificant GDP contractions. A shortcoming of this approach is that it is silent about the damages that the economy inflicts upon itself through the changes in temperatures it brings about – precisely what we understand as the damages from anthropological global warming. We propose to bridge this gap with a counterfactual exercise, loosely inspired by Mountford & Uhlig (2009), McKay & Wolf (2023) and Ciccarelli & Marotta (2024). To implement this, ideally we would want to compare the IRF of GDP to the expansionary shock in the data to a counterfactual where temperatures are unaffected by the expansion and therefore cannot spill back into the economy. Given the rich geographic heterogeneity of our data set this poses a substantial complication: temperatures should not react anywhere, which would require nullifying the 3,325 IRFs of US temperatures. This is clearly not possible. We therefore compute the counterfactual as the best possible approximation to a zero response everywhere in the country. In this context, the typical SVAR counterfactual exercise consists in finding a sequence of structural shocks (whose IRFs are known), which pushes the temperature IRFs after the expansionary shocks as close as possible to the zero line. Since this sequence of shocks can involve very large or strongly correlated shocks, it is subject to the Lucas Critique. As a solution to this, McKay & Wolf (2023) propose to use several structural shocks to impose the desired temperature path instead, but let the shocks hit only once.

In the context of our empirical model, this implies the following steps: first, identify the three economic shocks as before and find the conditional temperature variance maximizers everywhere in the US. We use five shocks for this, namely the maximizers of high- and business cycle frequencies as these are less prone to interference from economic shocks, US-based or international, than low frequency drivers. Next, collect the associated columns of  $H$  in the matrix  $H_c$ . Call the structural responses of  $Y_t$  to these shocks  $P(L) = D(L)H_c$ . Second, for a given economic shock vector  $u^E$ , find the corresponding temperature shocks  $u^T$  which minimize the responses of temperatures over the horizons  $j = 1, \dots, J$  at all locations  $i = 1, \dots, N$ .  $u^E$  is in our case a  $3 \times 1$  vector whose elements are zeros except for a one in the position of the current economic shock of interest. After this, recompute the implied IRFs. Formally, we ideally want to achieve:

$$\Lambda P_j^E u^E + \Lambda P_j^T u^T = \mathbf{0}_N \quad \forall j$$

where the superscript  $E$  implies picking the columns related to the economic shocks and analogously for  $T$  and temperatures. That is, the response to all shocks in the system described by  $H_c$  of temperatures everywhere should be zero at all impulse response horizons. This is not possible, because there are  $N \times J$  conditions and far fewer shocks. Therefore, we solve a least-squares problem which minimizes the error  $e_j$  between the temperature IRFs with and without  $u^T$ :

$$\Lambda P_j^E u^E + \Lambda P_j^T u^T = e_j \quad \forall j$$

The objective is then to minimize the sum of the sums of squared errors over all grid cells and all horizons:

$$\hat{u}^T = \arg \min_{u^T} \sum_{j=0}^J e'_j e_j = \arg \min_{u^T} \sum_{j=0}^J (\Lambda P_j^E u^E + \Lambda P_j^T u^T)' (\Lambda P_j^E u^E + \Lambda P_j^T u^T) \quad (13)$$

The closed form solution of this is given by

$$\hat{u}^T = - \left( \sum_{j=0}^J (\Lambda P_j^T)' (\Lambda P_j^T) \right)^{-1} \left( \sum_{j=0}^J (\Lambda P_j^T)' (\Lambda P_j^E u^E) \right) \quad (14)$$

We can then compute the counterfactual IRFs ( $IRF_c$ ) to the economic shock of interest that occurs simultaneously with the weather shocks that implement the desired path of US temperatures as best as possible from  $IRF_c = P(L)[u^E, \hat{u}^T]'$ .

**Figure 14:** Counterfactual IRFs of real GDP to the three economic shocks with temperature responses across the US muted to zero.

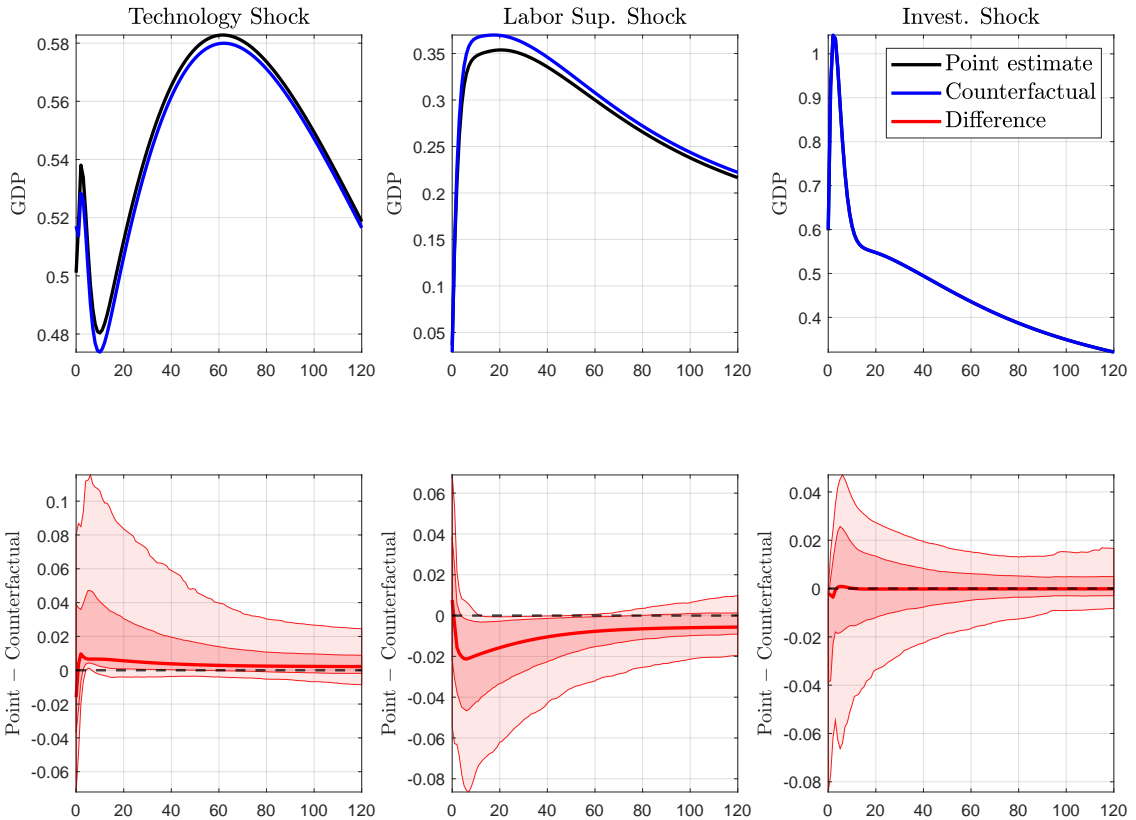


Figure 14 reports the results of this exercise. The differences in the paths are very small, in the order of  $-0.02\%$  to  $-0.006\%$  for the labor supply shock,  $-0.004\%$  to  $-0.0001\%$  for the investment shock and about  $0.01$  to  $0.002\%$  for the technology shock, where in each case the latter number refers to the period after 30 years. Given that the temperature IRFs after the expansionary shocks are already very close to zero, the shocks necessary to bring them even closer are quite small, around  $9\%$ ,  $7\%$ , and  $4\%$  of a standard deviation for the respective shocks. The reduction in distance towards zero over the full horizon is  $-58\%$ ,  $-31\%$  and  $-12\%$  for the three shocks with respect to the baseline estimates. Nevertheless, the signs of the differences suggest that if there were no spillback from temperature changes into the economy after an expansionary shock, output would generally be higher than what we measure in the true data. A policy that was able to achieve this outcome would still (in non-discounted terms) save between  $0.02$  (investment shock) and  $3.9$  (labor supply) billion dollars if the shock occurred in 2017.

## 6 Conclusion

We model an empirical joint climate-economic system to investigate the effect of economic shocks on temperatures in the US and vice versa. Using the principal components of a large, gridded data set of US temperatures we show that at least five shocks are necessary to accurately reflect temperature variations of different frequencies everywhere in the contiguous US, calling into question papers that use a single “climate shock” or focus on cross-sectional averages to reflect temperature warming. We show that a clear connection between economy and temperatures exists, which is mostly driven by changes in TFP. We identify three economic shocks, arguably responsible for the bulk of business-cycle and long-term variation in the US economy and thus emissions of climate-active gases – a technology shock, a labor supply shock, and an investment shock. Identification in the frequency domain allows us to mix medium term and long-term identification assumptions. There is clear evidence that economic activity has affected US temperatures. Together the three shocks account for around  $25\%$  of the low frequency component of US temperatures. Investment shocks increase temperatures on average, technology shocks decrease them, and we explore the reasons for this by showing a significant role for aerosol emissions that induce local, short-lived cooling and GHG emissions that lead to slow-paced, encompassing warming.

On the other hand, the economic damages from changing temperatures are small and come with substantial uncertainty. We show that temperature changes that affect primarily the US west coast lead to small economic expansions, as they are accompanied by decreasing temperatures in the east and south. Shocks raising temperatures elsewhere are mildly recessionary. We conduct a counterfactual exercise, through which we assess by how much output would change if temperature shocks could be recombined to minimize any endogenous temperature response to an economic expansion in the US. We find that for the labor supply shock and the investment shock output would be higher in the absence of temperature feedback. However, in monetary terms, the gains from cutting the link between the economy and temperatures is minimal for the US, suggesting that it has been well adapted to climate feedback in the past.

- Acevedo, S., Mrkaic, M., Novta, N., Pugacheva, E., & Topalova, P. (2020). The effects of weather shocks on economic activity: what are the channels of impact? *Journal of Macroeconomics*, 65, 103207.
- Alessi, L., Barigozzi, M., & Capasso, M. (2010). Improved penalization for determining the number of factors in approximate factor models. *Statistics & Probability Letters*, 80(23-24), 1806–1813.
- Angeletos, G.-M., Collard, F., & Dellas, H. (2020). Business-cycle anatomy. *American Economic Review*, 110(10), 3030–70.
- Annicchiarico, B., Carattini, S., Fischer, C., & Heutel, G. (2021). Business cycles and environmental policy: Literature review and policy implications.
- Auclert, A., Rognlie, M., & Straub, L. (2020). Micro jumps, macro humps: Monetary policy and business cycles in an estimated hank model. *National Bureau of Economic Research*.
- Barreca, A., Clay, K., Deschênes, O., Greenstone, M., & Shapiro, J. S. (2015). Convergence in adaptation to climate change: Evidence from high temperatures and mortality, 1900–2004. *American Economic Review*, 105(5), 247–251.
- Barsky, R. B., & Sims, E. R. (2011). News shocks and business cycles. *Journal of monetary Economics*, 58(3), 273–289.
- Bastien-Olvera, B. A., Granella, F., & Moore, F. C. (2022). Persistent effect of temperature on gdp identified from lower frequency temperature variability. *Environmental Research Letters*, 17(8).
- Bennedsen, M., Hillebrand, E., & Koopman, S. J. (2021). Modeling, forecasting, and nowcasting us co2 emissions using many macroeconomic predictors. *Energy Economics*, 96, 105118.
- Ben Zeev, N., & Khan, H. (2015). Investment-specific news shocks and us business cycles. *Journal of Money, Credit and Banking*, 47(7), 1443–1464.
- Berg, K. A., Curtis, C. C., & Mark, N. (2023). Gdp and temperature: Evidence on cross-country response heterogeneity. *National Bureau of Economic Research*.
- Bernanke, B. S., Boivin, J., & Eliasz, P. (2005). Measuring the effects of monetary policy: a factor-augmented vector autoregressive (favar) approach. *The Quarterly journal of economics*, 120(1), 387–422.
- Burke, M., Hsiang, S. M., & Miguel, E. (2015). Global non-linear effect of temperature on economic production. *Nature*, 527(7577), 235–239.
- Cai, Y., & Lontzek, T. S. (2019). The social cost of carbon with economic and climate risks. *Journal of Political Economy*, 127(6), 2684–2734.
- Carleton, T., Jina, A., Delgado, M., Greenstone, M., Houser, T., Hsiang, S., ... others (2022). Valuing the global mortality consequences of climate change accounting for adaptation costs and benefits. *The Quarterly Journal of Economics*, 137(4), 2037–2105.
- Ciccarelli, M., & Marotta, F. (2024). Demand or supply? an empirical exploration of the effects of climate change on the macroeconomy. *Energy Economics*, 129, 107163.
- Colacito, R., Hoffmann, B., & Phan, T. (2019). Temperature and growth: A panel analysis of the united states. *Journal of Money, Credit and Banking*, 51(2-3), 313–368.

- Conley, A., Westervelt, D., Lamarque, J.-F., Fiore, A., Shindell, D., Correa, G., ... Horowitz, L. (2018). Multimodel surface temperature responses to removal of us sulfur dioxide emissions. *Journal of Geophysical Research: Atmospheres*, 123(5), 2773–2796.
- de Juan, A., Poncela, P., Rodríguez-Caballero, V., & Ruiz, E. (2022). Economic activity and climate change. *arXiv preprint arXiv:2206.03187*.
- Dell, M., Jones, B. F., & Olken, B. A. (2012). Temperature shocks and economic growth: Evidence from the last half century. *American Economic Journal: Macroeconomics*, 4(3), 66–95.
- Deryugina, T., & Hsiang, S. M. (2014). Does the environment still matter? daily temperature and income in the united states. *National Bureau of Economic Research*.
- Deschênes, O., & Greenstone, M. (2007). The economic impacts of climate change: evidence from agricultural output and random fluctuations in weather. *American economic review*, 97(1), 354–385.
- DiCecio, R., & Owyang, M. (2010). Identifying technology shocks in the frequency domain. *Federal Reserve Bank of St. Louise Working Paper No.*
- Dieppe, A., Francis, N., & Kindberg-Hanlon, G. (2021). The identification of dominant macroeconomic drivers: coping with confounding shocks. *ECB Working Paper, No. 2021/2534*.
- Donadelli, M., Jüppner, M., Riedel, M., & Schlag, C. (2017). Temperature shocks and welfare costs. *Journal of Economic Dynamics and Control*, 82, 331–355.
- Erichson, N. B., Zheng, P., Manohar, K., Brunton, S. L., Kutz, J. N., & Aravkin, A. Y. (2020). Sparse principal component analysis via variable projection. *SIAM Journal on Applied Mathematics*, 80(2), 977–1002.
- Fernald, J. (2014). A quarterly, utilization-adjusted series on total factor productivity. *Federal Reserve Bank of San Francisco Working Paper, No. 2012/19*.
- Forni, M., Gambetti, L., Antonio, G., Sala, L., & Soccorsi, S. (2023). An american macroeconomic picture. *mimeo*.
- Forni, M., Gambetti, L., & Sala, L. (2014). No news in business cycles. *The Economic Journal*, 124(581), 1168–1191.
- Forni, M., Giannone, D., Lippi, M., & Reichlin, L. (2009). Opening the black box: Structural factor models with large cross sections. *Econometric Theory*, 25(5), 1319–1347.
- Foroni, C., Furlanetto, F., & Lepetit, A. (2018). Labor supply factors and economic fluctuations. *International Economic Review*, 59(3), 1491–1510.
- Forster, P. M., Forster, H. I., Evans, M. J., Gidden, M. J., Jones, C. D., Keller, C. A., ... others (2020). Current and future global climate impacts resulting from covid-19. *Nature Climate Change*, 10(10), 913–919.
- Fosten, J. (2019). Co2 emissions and economic activity: A short-to-medium run perspective. *Energy Economics*, 83, 415–429.
- Francis, N., & Ramey, V. A. (2009). Measures of per capita hours and their implications for the technology-hours debate. *Journal of Money, credit and Banking*, 41(6), 1071–1097.
- Gali, J. (1999). Technology, employment, and the business cycle: do technology shocks explain aggregate fluctuations? *American economic review*, 89(1), 249–271.
- Goulet Coulombe, P., & Göbel, M. (2021). On spurious causality, co2, and global temperature. *Econometrics*, 9(3), 33.

- Gourio, F., & Fries, C. (2020). Adaptation and the cost of rising temperature for the us economy. *mimeo*.
- Greene, C. A., Thirumalai, K., Kearney, K. A., Delgado, J. M., Schwanghart, W., Wolfenbarger, N. S., ... Blankenship, D. D. (2019). The climate data toolbox for MATLAB. *Geochemistry, Geophysics, Geosystems*. Retrieved from <https://doi.org/10.1029/2019GC008392> doi: 10.1029/2019GC008392
- Hannachi, A., Jolliffe, I. T., & Stephenson, D. B. (2007). Empirical orthogonal functions and related techniques in atmospheric science: A review. *International Journal of Climatology: A Journal of the Royal Meteorological Society*, 27(9), 1119–1152.
- Hsiang, S., Kopp, R., Jina, A., Rising, J., Delgado, M., Mohan, S., ... others (2017). Estimating economic damage from climate change in the united states. *Science*, 356(6345), 1362–1369.
- IPCC. (2023). Ar6 synthesis report: Climate change 2023. <https://www.ipcc.ch/report/sixth-assessment-report-cycle/>.
- Jones, M. W., Peters, G. P., Gasser, T., Andrew, R. M., Schwingshackl, C., Gütschow, J., ... Le Quéré, C. (2023). National contributions to climate change due to historical emissions of carbon dioxide, methane, and nitrous oxide since 1850. *Scientific Data*, 10(1), 155.
- Joos, F., Roth, R., Fuglestvedt, J. S., Peters, G. P., Enting, I. G., Von Bloh, W., ... others (2013). Carbon dioxide and climate impulse response functions for the computation of greenhouse gas metrics: a multi-model analysis. *Atmospheric Chemistry and Physics*, 13(5), 2793–2825.
- Jordà, O. (2005). Estimation and inference of impulse responses by local projections. *American economic review*, 95(1), 161–182.
- Justiniano, A., Primiceri, G. E., & Tambalotti, A. (2010). Investment shocks and business cycles. *Journal of Monetary Economics*, 57(2), 132–145.
- Justiniano, A., Primiceri, G. E., & Tambalotti, A. (2011). Investment shocks and the relative price of investment. *Review of Economic Dynamics*, 14(1), 102–121.
- Kahn, M. E., Mohaddes, K., Ng, R. N., Pesaran, M. H., Raissi, M., & Yang, J.-C. (2021). Long-term macroeconomic effects of climate change: A cross-country analysis. *Energy Economics*, 104, 105624.
- Kaufmann, R. K., Kauppi, H., Mann, M. L., & Stock, J. H. (2013). Does temperature contain a stochastic trend: linking statistical results to physical mechanisms. *Climatic change*, 118, 729–743.
- Khan, H., Metaxoglou, K., Knittel, C. R., & Papineau, M. (2019). Carbon emissions and business cycles. *Journal of Macroeconomics*, 60, 1–19.
- Kilian, L. (1998). Small-sample confidence intervals for impulse response functions. *Review of economics and statistics*, 80(2), 218–230.
- Kunkel, K. E., Stevens, L. E., Stevens, S. E., Sun, L., Janssen, E., Wuebbles, D., ... others (2013). Regional climate trends and scenarios for the us national climate assessment: Part 2. climate of the southeast us.
- Magnus, J. R., Melenberg, B., & Muris, C. (2011). Global warming and local dimming: The statistical evidence. *Journal of the American Statistical Association*, 106(494), 452–464.
- Mar, K. A., Unger, C., Walderdorff, L., & Butler, T. (2022). Beyond co2 equivalence: The impacts of methane on climate, ecosystems, and health. *Environmental science & policy*, 134, 127–136.

- Matsuura, K., & Willmott, C. J. (2018). Terrestrial air temperature: 1900–2017 gridded monthly time series. *University of Delaware, Newark, DE*. Retrieved from [http://climate.geog.udel.edu/~climate/html\\_pages/download.html#T2017](http://climate.geog.udel.edu/~climate/html_pages/download.html#T2017)
- McKay, A., & Wolf, C. K. (2023, September). What can time-series regressions tell us about policy counterfactuals? *Econometrica*, 91(5), 1695–1725.
- Montamat, G., & Stock, J. H. (2020). Quasi-experimental estimates of the transient climate response using observational data. *Climatic Change*, 160(3), 361–371.
- Mountford, A., & Uhlig, H. (2009). What are the effects of fiscal policy shocks? *Journal of applied econometrics*, 24(6), 960–992.
- Mumtaz, H., & Marotta, F. (2023). Vulnerability to climate change. evidence from a dynamic factor model. *mimeo*.
- Nath, I. B., Ramey, V. A., & Klenow, P. J. (2023). How much will global warming cool global growth? *Working paper*.
- Natoli, F. (2022). Temperature surprise shocks. *mimeo*.
- Natoli, F. (2023). The macroeconomic effects of temperature surprise shocks. *Available at SSRN 4160944*.
- Newell, R. G., Prest, B. C., & Sexton, S. E. (2021). The gdp-temperature relationship: implications for climate change damages. *Journal of Environmental Economics and Management*, 108, 102445.
- NOAA. (2023). What are la niña and el niño and why do they matter? *ENSO Fact Sheet*. Retrieved from <https://www.ipcc.ch/report/sixth-assessment-report-cycle/>
- Peersman, G., & Straub, R. (2009). Technology shocks and robust sign restrictions in a euro area svar. *International Economic Review*, 50(3), 727–750.
- Phillips, P. C., Leirvik, T., & Storelvmo, T. (2020). Econometric estimates of earth's transient climate sensitivity. *Journal of Econometrics*, 214(1), 6–32.
- Pretis, F. (2020). Econometric modelling of climate systems: The equivalence of energy balance models and cointegrated vector autoregressions. *Journal of Econometrics*, 214(1), 256–273.
- Pretis, F. (2021). Exogeneity in climate econometrics. *Energy Economics*, 96, 105122.
- Ramey, V. A. (2016). Macroeconomic shocks and their propagation. *Handbook of macroeconomics*, 2, 71–162.
- Ricke, K. L., & Caldeira, K. (2014). Maximum warming occurs about one decade after a carbon dioxide emission. *Environmental Research Letters*, 9(12), 124002.
- Shapiro, M. D., & Watson, M. W. (1988). Sources of business cycle fluctuations. *NBER Macroeconomics annual*, 3, 111–148.
- Smith, S. J., van Aardenne, J., Klimont, Z., Andres, R. J., Volke, A., & Delgado Arias, S. (2011). Anthropogenic sulfur dioxide emissions: 1850–2005. *Atmospheric Chemistry and Physics*, 11(3), 1101–1116.
- Stock, J. H. (2020). Climate change, climate policy, and economic growth. *NBER Macroeconomics Annual*, 34(1), 399–419.
- Storelvmo, T., Leirvik, T., Lohmann, U., Phillips, P. C., & Wild, M. (2016). Disentangling greenhouse warming and aerosol cooling to reveal earth's climate sensitivity. *Nature Geoscience*, 9(4), 286–289.
- Uhlig, H. (2003). What drives gnp? *Unpublished manuscript, Euro Area Business Cycle Network*.

Zickfeld, K., & Herrington, T. (2015). The time lag between a carbon dioxide emission and maximum warming increases with the size of the emission. *Environmental Research Letters*, 10(3), 031001.

## Appendix A: Data construction

We follow Angeletos et al. (2020) in constructing the economic variables.

**Table 5:** Economic Data Sources and Transformations

Data	FRED Mnemonic	Frequency/Transformation
Real gross domestic product per capita	A939RX0Q048SBEA	Q
Real Gross domestic product	GDPC1	Q
Share of GDP: gross private domestic investment	A006RE1Q156NBEA	Q
Share of GDP: personal consumption expenditures: durable goods	DDURRE1Q156NBEA	Q
Nonfarm business sector: average weekly hours	PRS85006023	Q
Employment Level	CE16OV	M2Q (EoP)
Total factor productivity (annualized Q-Q growth rate)	dTFPu (from Fernald)	Q

The variables enter the model as follows:

1. **Real GDP:**  $\log(GDPC1) \times 100$
2. **Real investment:**  
 $\log((DDURRE1Q156NBEA + A006RE1Q156NBEA) \times GDPC1) \times 100$
3. **Hours:**  $\log(PRS85006023 \times CE16OV) \times 100$
4. **TFP:**  $\text{cumsum}(dTFPu/400) \times 100$
5. **Population:**  $GDPC1/A939RX0Q048SBEA$

For checks, the variables real GDP, real investment, and hours can be transformed to per capita units by dividing by the population level as computed above before taking logs.

## Appendix B: Bootstrap procedure

We compute confidence bands for the IRFs and the cyclical variances using the following bootstrap procedure:

1. Use (2) to generate a new vector  $Y_t$  by bootstrapping from the reduced form residuals.
2. Use the method of Kilian (1998) to correct the bias of the OLS estimates.
3. Use  $\Lambda$  to recompute the common component of temperatures,  $\Lambda Y_t$ , and add the original idiosyncratic component,  $\eta_{it}$ , to get a new data set of US temperatures.
4. On this new data set, estimate  $r = 8$  principal components, and re-estimate a bootstrap  $\Lambda^B$ .
5. Estimate the FAVAR in (2) again with  $p = 2$ .
6. Identify the shocks sequentially, compute IRFs and the cyclical variances.
7. Repeat this 1,500 times to obtain bootstrap distributions of the IRFs and the cyclical variances.
8. Find the quantiles of the bootstrap distributions to get the 68% and 90% intervals.

## Appendix C: Robustness checks

To test the sensitivity of our results to the underlying assumptions we conduct the following robustness checks:

### *1. Changing the number of temperature factors:*

We have used a statistical criterion to determine the number of factors to be extracted from the gridded temperature data set and opted for  $r = 8$  in our preferred specification for parsimony. The upper bound recommended by the criterion was  $r = 17$ , which we test. In this case we set  $p = 1$  according to the BIC.

### *2. More lags:*

Our results concern mostly the low frequency components of temperatures. There may be reason to believe that this is inaccurately reflected in our model if the lag length is very short. In the baseline specification we had used  $p = 2$ . We increase this to  $p = 4$  as a check. Given the frequentist approach to estimation, results become quite erroneous for even larger lag orders.

### *3. Sub-sample analysis 1970:*

We have used data between 1948 and 2017. The trend in temperatures that is usually attributed to human influence becomes very pronounced in our data as of around 1970. Moreover, as of the 1970s, SO<sub>2</sub> emissions in the US start to decline. We repeat our exercise by excluding the first 22 years from the sample.

### *4. Potential interference from outside shocks:*

There may be non-US shocks driving BC and LF variation in US aggregates that then affect temperatures. While the US is usually treated as having frontier technology (Nath et al., 2023). It may be that shocks in China spill over to the US and then show up as US shocks affecting temperatures when really the origin is elsewhere. Long quarterly time series for China are difficult to obtain, but annual series for CO<sub>2</sub> emissions show an impressive uptick as of the year 2000. We therefore cut the sample at Q4:1999 to check if our results obscure external influences from China.

### *5. Maximizing long-run IRFs instead of variances:*

An alternative to maximizing variances is represented by maximizing the long-run IRF of TFP (and hours). This is used, for example, in Forni et al. (2014). Since the connection between the economy and temperatures appears to run largely through TFP, correct identification of the technology shock is crucial.

### *6. Variables in per capita terms:*

Long-run economic dynamics may be affected by demographic sources (Francis & Ramey, 2009) which we are not taking explicitly into account in our baseline specification. Population changes are an important source of emission variations according to the *Kaya identity*. We therefore check, whether expressing the economic variables GDP, hours and investment in per capita terms changes our results.

### *Robustness results:*

The results are insensitive to the selection of the lag order, number of factors or specification of variables in per-capita terms. Minor changes obtain for sub samples and when altering the long-run identification assumption as in robustness check 5. Figure 15 shows the IRFs for average US temperatures to the economic shocks. The most significant differences arise when we change the sub-samples to post 1970 and pre-2000, as then the technology shock leads to positive temperature responses. This is because the role of SO<sub>2</sub> emissions and other aerosols in depressing temperatures is diminished after 1970. Similarly, excluding the more recent period from the sample attributes some cooling to the investment shock as the reduction on SO<sub>2</sub> emissions has not yet materialized. While these changes are interesting, we rather see them as further evidence for the importance of this additional channel for the transmission of economic activity to temperature changes.

**Figure 15:** Impulse response functions of US average temperatures to economic shocks for robustness checks 1-6.

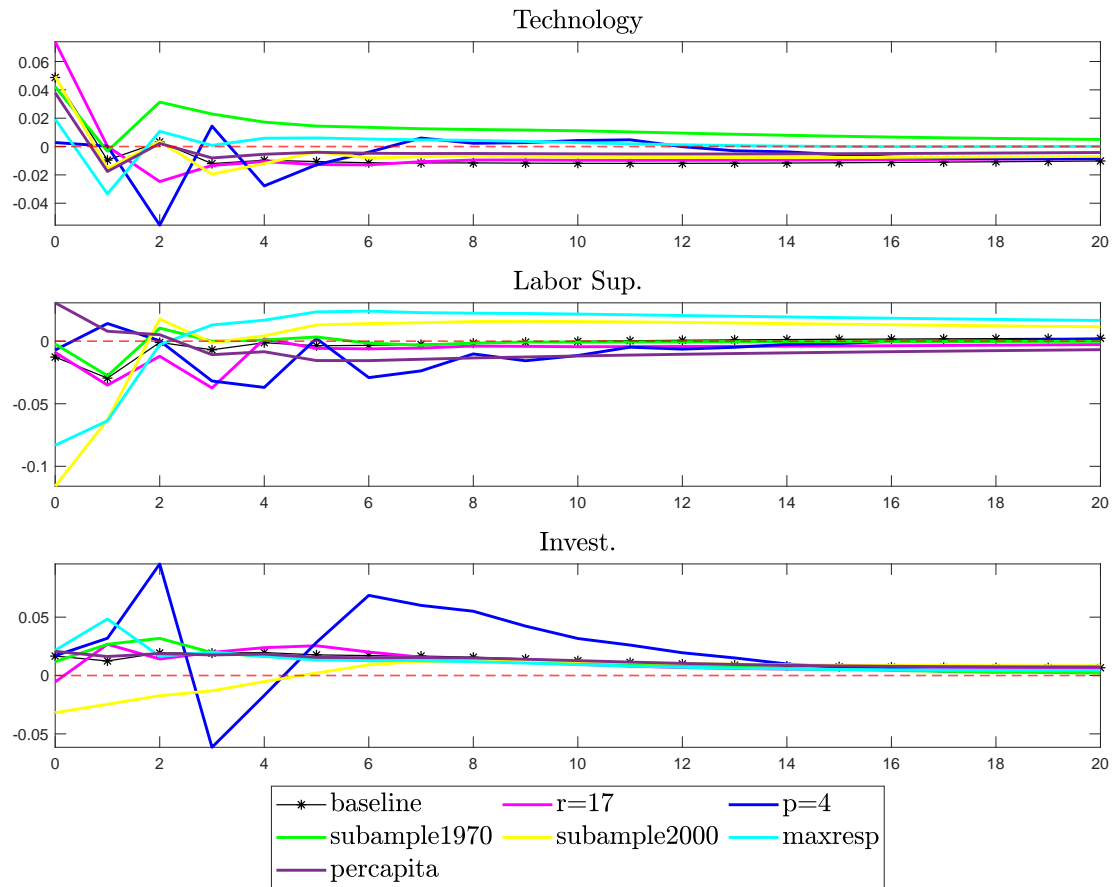
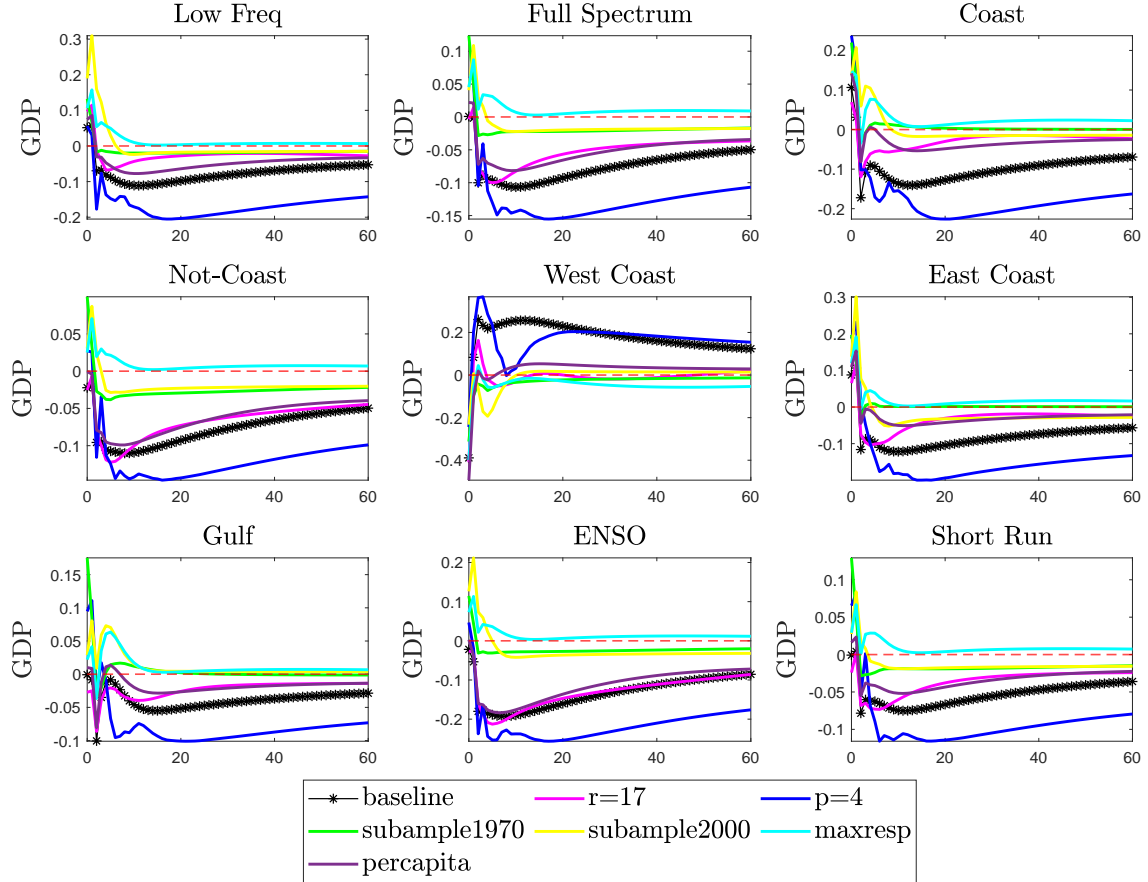


Figure 16, on the other hand, reports the IRFs of real GDP to the different temperature shocks for all robustness checks. We observe that changing the number of temperature principal components or the number of lags has negligible effects on the IRFs compared to our baseline specification. The same goes for taking the variables in per capita terms. Changes in the responses of GDP to the temperature shocks are slightly more pronounced if we use labor productivity instead of TFP or the maximal response identification strategy to obtain the technology shock and then condition the temperature shocks on it. All in all, the baseline specification lies roughly in the middle of the IRFs under the different

robustness checks. We leave the robustness check IRFs of the economic variables to the economic shocks in the Appendix since the only minor difference arises when using the response maximization approach over the cyclical variance maximization approach.

**Figure 16:** Impulse response functions of GDP to temperature shocks for robustness checks 1-6.



**Figure 17:** Impulse response functions of economic variables to economic shocks for robustness checks 1-6.

